

Multiple Testing of Local Extrema for Detection of Structural Breaks in Piecewise Linear Models

Zhibing He

Department of Biostatistics, Yale University

Dan Cheng *

Department of Statistics, Arizona State University
and

Yunpeng Zhao

Department of Statistics, Colorado State University

Abstract

In this paper, we propose a new generic method for detecting the number and locations of structural breaks or change points in piecewise linear models under stationary Gaussian noise. Our method transforms the change point detection problem into identifying local extrema through kernel smoothing and differentiation of the data sequence. By computing p-values for all local extrema based on the derived peak height distributions of derivatives of smooth Gaussian processes, we utilize the Benjamini-Hochberg procedure to identify significant local extrema as the detected change points. Our method effectively distinguishes between two types of change points: continuous breaks (Type I) and jumps (Type II). We study three scenarios of piecewise linear signals: pure Type I, pure Type II and a mixture of both. The results demonstrate that our proposed method ensures asymptotic control of the False Discover Rate (FDR) and power consistency, as sequence length, slope changes, and jump size increase. Furthermore, compared to traditional change point detection methods based on recursive segmentation, our approach requires only one instance of multiple-testing across all candidate local extrema, thereby achieving the smallest computational complexity proportionate to the data sequence length. Additionally, numerical studies illustrate that our method maintains FDR control and power consistency, even in non-asymptotic situations with moderate slope changes or jumps. We have implemented our method in the R package “dSTEM” (available from <https://cran.r-project.org/web/packages/dSTEM>).

Keywords: structural breaks, change points, piecewise linear models, kernel smoothing, multiple testing, Gaussian processes, peak height distribution, FDR, power consistency.

*Corresponding author. Email: chengdan@asu.edu

1 Introduction

In this paper, we consider a canonical univariate statistical model:

$$y(t) = \mu(t) + z(t), \quad t \in \mathbb{R}, \quad (1)$$

where $z(t)$ is correlated stationary Gaussian noise and $\mu(t)$ is a piecewise linear signal of the form

$$\mu(t) = c_j + k_j t, \quad t \in (v_{j-1}, v_j],$$

where $c_j, k_j \in \mathbb{R}$, $j = 1, 2, \dots$ and $-\infty = v_0 < v_1 < v_2 < \dots$. Assume the structures of $\mu(t)$ are different at neighboring v_j , i.e., $(c_j, k_j) \neq (c_{j+1}, k_{j+1})$, resulting in a continuous break or jump at v_j (see figure 1). Such v_j is called a change point or structural break.

The detection of structural breaks or change points plays a pivotal role in various fields, including statistics, econometrics, genomics, climatology and medical imaging. These detection methods are broadly applied to different domains based on different types of signals. For instance, in medical condition monitoring (Khan et al., 2020; Hann et al., 2009; Bulut et al., 2005) and image analysis (Liao and Pawlak, 1996; Kharinov, 2014), the presence of piecewise constant signals with jumps can indicate significant changes in patients' health conditions or object characteristics in images. Accurate detection of these changes is paramount for aiding in diagnosis, treatment planning, and object recognition tasks. On the other hand, piecewise linear signals with continuous breaks are commonly encountered in climate change research (Tomé and Miranda, 2004; Tebaldi and Lobell, 2008) and human activity analysis (Van Laerhoven et al., 2009; Lu et al., 2019). These changes may represent gradual shifts in temperature patterns or human behavior. Additionally, in financial markets, piecewise linear signals with noncontinuous breaks may indicate sudden shifts in stock prices or market dynamics (Chang et al., 2008; Ding et al., 2010). Monitoring and detecting these changes are crucial for making informed investment decisions and predicting market trends.

To differentiate between various ways of linear structure changes, we define the following two types of change points:

Definition 1. A point v_j is called a *Type I change point (structural break)* if $c_j + k_j v_j = c_{j+1} + k_{j+1} v_j$ and $k_j \neq k_{j+1}$, and a point v_j is denoted as a *Type II change point* if $c_j + k_j v_j \neq c_{j+1} + k_{j+1} v_j$ for $j \geq 1$.

At Type I change points v_j , the signals remain continuous, but the slopes experience a sudden change at v_j . Type II change points correspond to jumps in the signal, where there is a discontinuity between adjacent segments. Note that, a special case of Type II change points is that $\mu(t)$ is piecewise constant, i.e., $k_j \equiv 0$ and $c_j \neq c_{j+1}$ for $j \geq 1$. In this paper, we specifically focus on three scenarios of the signal $\mu(t)$, each representing different characteristics of change points. The scenarios are described as follows:

Scenario 1: Pure Type I Change Points. The signal $\mu(t)$ consists of continuous segments with slope changes at specific points v_j . Figure 1 (a) illustrates this scenario, where the signal exhibits continuous behavior with distinct slopes at the change points.

Scenario 2: Pure Type II Change Points. The signal $\mu(t)$ contains only Type II change points (jumps). Figure 1 (d) illustrates this scenario, where the signal exhibits sudden changes or discontinuities at change points.

Scenario 3: Mixture of Type I and Type II Change Points. The signal $\mu(t)$ combines both continuous breaks (Type I) and jumps (Type II) Figure 1 (g) illustrates this scenario, where it allows for a more general and realistic representation of signals with mixed characteristics.

In this paper, our primary objective is to detect both the number of change points and their locations simultaneously. To address this problem, we propose a novel and generic approach that can handle an unknown number of multiple structural breaks occurring at unknown positions within the signal. Our proposed method for change point detection is illustrated and evaluated in three aforementioned scenarios (pure Type I change points, pure Type II change points, and a mixture of Type I and Type II change points). Figure 1 shows the application of our method to each scenario, showcasing the mechanism behind our change point detection method.

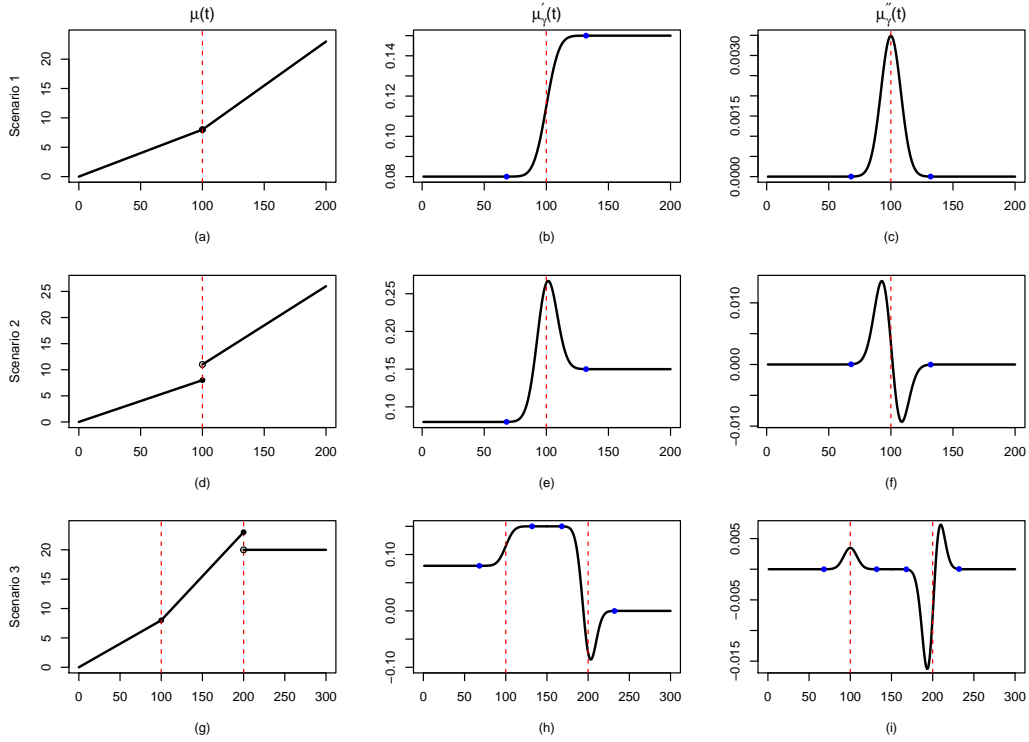


Figure 1: Illustration of change point detection. A change point in the piecewise linear signal $\mu(t)$ (left panel) becomes a local extremum in either the first derivative of the smoothed signal $\mu'_{\gamma}(t)$ (middle panel) or in the second derivative of the smoothed signal $\mu''_{\gamma}(t)$ (right panel). The red dashed lines indicate the locations of true change points, and the blue points represent the regions where the signal is smoothed using a Gaussian kernel. The top row shows a Type I change point v_j in $\mu(t)$ becomes a local extremum in $\mu''_{\gamma}(t)$ precisely at $t = v_j$. The middle row illustrates a Type II change point v_j in $\mu'_{\gamma}(t)$ becomes a local extremum in $\mu''_{\gamma}(t)$ around v_j . The bottom row shows that only Type II change points can generate local extrema in $\mu'_{\gamma}(t)$, whereas both Type I and Type II change points can generate local extrema in $\mu''_{\gamma}(t)$.

The key idea behind our approach is based on the observation that a change point in the signal $\mu(t)$ will manifest as a local extremum (local maximum or local minimum) in either the first or second derivative of the smoothed signal. By kernel smoothing and differentiating the data sequence, we transform the problem of change point detection into identifying local extrema. Specifically,

- (i) A Type I change point in $\mu(t)$ becomes a local extremum in the second derivative $\mu''_{\gamma}(t)$ (see Figure 1 (a) and (c)).
- (ii) A Type II change point in $\mu(t)$ becomes a local extremum in the first derivative $\mu'_{\gamma}(t)$ (see Figure 1 (d) and (e)).

Therefore, in Scenario 1 and Scenario 2, the detection of change points relies on identifying local extrema in the second and the first derivatives of the smoothed signal respectively. However, in Scenario 3 a different approach is required due to the unique characteristics of each type:

- Type I change points do not generate local extrema in the first derivative $\mu'_{\gamma}(t)$ (see Figure 1 (b)). Therefore, in Scenario 3, the detection process begins by identifying all Type II change points as local extrema in $\mu'_{\gamma}(t)$.
- On the other hand, local extrema in the second derivative $\mu''_{\gamma}(t)$ can be generated by both Type I and Type II change points (see Figure 1 (i)). To detect Type I change points in Scenario 3, one needs to remove the local extrema in $\mu''_{\gamma}(t)$ generated by Type II change points.

By combining these approaches, our proposed method can distinguish between Type I and Type II change points in Scenario 3.

The detection of local extrema can be formulated as a peak detection problem, focusing on the local extrema of the first and second derivatives. In the literature, there have been notable contributions addressing this issue. One such notable approach is the Smoothing and TEsting of Maxima (STEM) algorithm (Schwartzman et al., 2011; Cheng and Schwartzman, 2017). The STEM algorithm aims to identify local maxima of the derivative as candidate peaks, which correspond to

potential change points in the signal. By kernel smoothing the signal and applying multiple testing, the algorithm distinguishes between local extrema generated by true change points and those arising from random noise. Moreover, [Cheng et al. \(2020\)](#) introduced the differential STEM (dSTEM) method specifically designed for detecting change points in data sequences modeled as a piecewise constant signal-plus-noise. The dSTEM method leverages the principles of the STEM algorithm but adapts it to the piecewise constant signal model. This modification allows for more effective change point detection in scenarios where the signal exhibits piecewise constant behavior.

Literature on change point detection contains a vast amount of research work of statistical inference, but most of it specially designed for the case of a single change point with unknown location. For example, for the case of a single change point with an unknown location, [Andrews \(1993\)](#) and [Andrews et al. \(1996\)](#) proposed comprehensive treatments and testing methods for structural change. [Perron \(1989\)](#) utilized unit root tests for detecting a one-time change in the level or slope of the trend function in univariate time series. [Bai \(1994\)](#) introduced the method of least squares for estimating an unknown shift point (change point) in a piecewise constant model. In recent years, there has been extensive interest in multiple change point detection, particularly in the context of multiple testing-based methods. In the piecewise constant signal model, [Yao and Au \(1989\)](#) studied least squares estimators for the locations and levels of the step function under both known and unknown numbers of jumps. [Lavielle \(2005\)](#) developed a penalized least squares method for estimating the number of change points and their locations. Binary segmentation (BS) ([Vostrikova, 1981](#)) is another popular approach, and [Hyun et al. \(2021\)](#) outlined similar post-selection tests for change point detection using Wild Binary Segmentation (WSB) ([Fryzlewicz, 2014](#)) and circular Binary Segmentation (CBS) ([Olshen et al., 2004](#)). SMUCE ([Frick et al., 2014](#); [Pein et al., 2017](#)) estimates the number of change points as the minimum among all candidate fits, where the empirical residuals pass a certain multi-scale test at a given significance level. [Li et al. \(2016\)](#) proposed an estimator that controls the False Discovery Rate (FDR) while allowing for a generous definition of a true discovery. FDR control was also demonstrated for the SaRa estimator ([Hao et al., 2013](#)) and

the dSTEM estimator (Cheng et al., 2020) for multiple change point locations. For general piecewise linear signal models, Bai and Perron (1998) provided asymptotic distribution results regarding the distance between estimated change points and their true locations, assuming a known number of change points and a minimum distance of $O(L)$. However, the distributional limits depend on the unknown magnitudes of parameter changes, which can be challenging to estimate accurately. Additionally, methods such as narrowest-over-threshold (NOT) (Baranowski et al., 2019) and narrowest significance pursuit (NSP) (Fryzlewicz, 2023) have been proposed to detect change points by focusing on localized regions that contain suspected features. These works represent a diverse range of approaches for change point detection, providing valuable insights and methodologies for addressing both single and multiple change point scenarios in various signal models.

In this paper, we propose a modified Smoothing and TEsting of Maxima (mSTEM) algorithm for the change point detection in piecewise linear models under stationary Gaussian noise. Our proposed approach is unique in comparison with the existing literature in following ways:

1. Simultaneous estimation of the number and locations of change points. Our method allows for the estimation of both the number and locations of change points in the data simultaneously. By identifying significant local extrema in the first or second derivative under a global significance level, we provide a new framework for change point detection.
2. Detecting separately Type I and Type II change points. Our method can effectively distinguish between Type I and Type II change points. This capability is particularly useful in practical scenarios where researchers might be specifically interested in detecting jumps (Type II) or continuous breaks (Type I).
3. Low computational complexity. Our proposed method achieves a significantly lower computational complexity compared to traditional change point detection methods. By testing only the candidate peaks generated by true change points or random noise once, the method reduces the computation to the number of candidate peaks, which proportionate to the length of

data sequence L . Thus our proposed method can achieve lowest computational complexity of $O(L)$. This is a significant advantage, as most existing methods typically have computational costs of $O(L^2)$. The binary segmentation (BS) based method can achieve a lower computational complexity of order $O(L \log L)$ (Fryzlewicz, 2014).

4. General form of peak height distribution. We derive a general and straightforward form of the peak height distribution for derivatives of Gaussian processes, which depends on only one parameter. This generalizes and extends those distributions used in Schwartzman et al. (2011) and Cheng et al. (2020).
5. Applications to correlated noise. Our method takes into account the presence of correlated noise by assuming that the noise follows a Gaussian process. This is an important contribution, as many real-world datasets exhibit correlated noise (Hung et al., 2013), and our approach expands the applicability of change point detection methods to such scenarios.

This paper is organised as follows. Section 2 introduces the framework of our change point detection method. Section 3 provides change point detection algorithms under different scenarios and their asymptotic theories. Section 4 provides the simulation studies for various signal settings. Two real data studies are described in Section 5. Section 6 concludes with a brief discussion.

2 The mSTEM detection framework

2.1 The kernel smoothed signal

Consider the model (1). The jump size a_j at v_j is defined as

$$a_j = c_{j+1} + k_{j+1}v_j - (c_j + k_jv_j) = (c_{j+1} - c_j) + (k_{j+1} - k_j)v_j, \quad j \geq 1. \quad (2)$$

By definition 1 a change point v_j is a Type I change point if $a_j = 0$ and a Type II change point if $a_j \neq 0$. Assume $d = \inf_j (v_j - v_{j-1}) > 0$ such that there is a minimal distance d between neighboring change points. In addition, we assume $k = \inf_j |k_{j+1} - k_j| > 0$ at Type I change

points and $a = \inf_j |a_j| > 0$ at Type II change points respectively such that the slope changes and jump sizes do not become arbitrarily small.

Denote by $\phi(x)$ and $\Phi(x)$ the pdf and cdf of the standard normal distribution, respectively. Let $w_\gamma(t)$ be the Gaussian kernel with compact support $[-c\gamma, c\gamma]$ (we set $c = 4$ throughout the paper) and bandwidth γ , i.e.,

$$w_\gamma(t) = \frac{1}{\gamma} \phi\left(\frac{t}{\gamma}\right) \mathbb{1}\{-c\gamma \leq t \leq c\gamma\}. \quad (3)$$

Convolving the signal-plus-noise process (1) with the kernel $w_\gamma(t)$ leads to the generation of a smoothed random process:

$$y_\gamma(t) = w_\gamma(t) * y(t) = \int_{\mathbb{R}} w_\gamma(t-s)y(s) ds = \mu_\gamma(t) + z_\gamma(t), \quad (4)$$

where the smoothed signal and smoothed noise are defined respectively as

$$\mu_\gamma(t) = w_\gamma(t) * \mu(t) \quad \text{and} \quad z_\gamma(t) = w_\gamma(t) * z(t).$$

The smoothed noise $z_\gamma(t)$ is assumed to be a zero-mean and four-times differentiable stationary ergodic Gaussian process. To avoid the overlap of smoothing two neighboring change points, we assume that $d = \inf_j (v_j - v_{j-1})$ is large enough, say greater than $2c\gamma$.

2.2 Local extrema for derivatives of the smoothed signal

For a smooth function $f(t)$, denote by $f^{(\ell)}(t)$ its ℓ -th derivative, $\ell \geq 1$, and write by default $f'(t) = f^{(1)}(t)$ and $f''(t) = f^{(2)}(t)$ respectively. We have the following derivatives of the smoothed observed process (4),

$$y_\gamma^{(\ell)}(t) = w_\gamma^{(\ell)}(t) * y(t) = \int_{\mathbb{R}} w_\gamma^{(\ell)}(t-s)y(s) ds = \mu_\gamma^{(\ell)}(t) + z_\gamma^{(\ell)}(t), \quad (5)$$

where the derivatives of the smoothed signal and smoothed noise are respectively

$$\mu_\gamma^{(\ell)}(t) = w_\gamma^{(\ell)}(t) * \mu(t) \quad \text{and} \quad z_\gamma^{(\ell)}(t) = w_\gamma^{(\ell)}(t) * z(t), \quad \ell \geq 1.$$

The following lemmas on the first and second derivatives of the smoothed signal $\mu_\gamma(t)$ are useful in characterizing the extrema (see Figure 1). The proofs are provided in the Appendix.

Lemma 1. *The first and second derivatives of $\mu_\gamma(t)$ over $(v_{j-1} + c\gamma, v_{j+1} - c\gamma)$ are given respectively by*

$$\mu'_\gamma(t) = \begin{cases} k_j[2\Phi(c) - 1], & t \in (v_{j-1} + c\gamma, v_j - c\gamma), \\ \frac{a_j}{\gamma}\phi\left(\frac{v_j-t}{\gamma}\right) + (k_j - k_{j+1})\Phi\left(\frac{v_j-t}{\gamma}\right) + (k_j + k_{j+1})\Phi(c) - k_j, & t \in (v_j - c\gamma, v_j + c\gamma), \\ k_{j+1}[2\Phi(c) - 1], & t \in (v_j + c\gamma, v_{j+1} - c\gamma); \end{cases}$$

$$\mu''_\gamma(t) = \begin{cases} \frac{a_j(v_j-t) + (k_{j+1}-k_j)\gamma^2}{\gamma^3}\phi\left(\frac{v_j-t}{\gamma}\right), & t \in (v_j - c\gamma, v_j + c\gamma), \\ 0, & \text{otherwise,} \end{cases}$$

where a_j is the jump size defined by (2).

Lemma 2. *The local extremum of $\mu'_\gamma(t)$ over $(v_j - c\gamma, v_j + c\gamma)$ is achieved at*

$$t = \begin{cases} v_j + \gamma^2 q_j, & \text{if } a_j \neq 0, \\ \text{does not exist,} & \text{if } a_j = 0; \end{cases} \quad (6a)$$

$$(6b)$$

while the local extremum of $\mu''_\gamma(t)$ over $(v_j - c\gamma, v_j + c\gamma)$ is achieved at

$$t = \begin{cases} v_j + \frac{1}{2} \left(\gamma^2 q_j \pm \gamma \sqrt{\gamma^2 q_j^2 + 4} \right), & \text{if } a_j \neq 0, \\ v_j, & \text{if } a_j = 0, \end{cases} \quad (7a)$$

$$(7b)$$

where $q_j = \frac{k_{j+1}-k_j}{a_j}$ for $a_j \neq 0$.

Recall that a_j is the size of jump at the change point v_j , thus v_j is a Type I change point if $a_j = 0$ and a Type II change point if $a_j \neq 0$. Note that q_j is the ratio between the change of slope and size of jump, and will be assumed to be small. It is seen that Lemma 2 characterizes the relation between the peak location of the differentiated smoothed signal and the original location v_j , yielding the following result.

Proposition 1. *A Type I change point v_j becomes a local extremum in $\mu''_\gamma(t)$ precisely at v_j (see (7b)); while a Type II change point v_j results in a local extremum in $\mu'_\gamma(t)$ at $v_j + \gamma^2 q_j$ (see (6a)), which tends to v_j as $q_j \rightarrow 0$.*

More specifically, as it can be seen from the proof that, a Type I change point v_j becomes a local maximum in $\mu''_\gamma(t)$ if $k_{j+1} - k_j > 0$ (a local minimum if $k_{j+1} - k_j < 0$); and a Type II change point v_j results in a local maximum in $\mu'_\gamma(t)$ near v_j if $a_j > 0$ (a local minimum if $a_j < 0$), regardless of the sign of $k_{j+1} - k_j$. Basically, Proposition 1 shows that the change points would be transformed to peaks in $\mu'_\gamma(t)$ or $\mu''_\gamma(t)$, providing the main idea on the detection in the pure cases Scenarios 1 and 2.

Remark 1. Based on the results in Lemma 2, here we discuss the idea on detecting separately Types I and II change points in Scenario 3 where both types of change points exist. This will be shown in more details in Algorithm 3 below.

First, note that a Type I change point does not generate any local extremum in $\mu'_\gamma(t)$ (see (6b)). This property is crucial to detect Type II change points via detecting peaks in $\mu'_\gamma(t)$ by Proposition 1 (see Step 1 in Algorithm 3). On the other hand, by (7a), a Type II change point v_j will generate a pair of local maximum and minimum in $\mu''_\gamma(t)$, with locations tending to $v_j \pm \gamma$ when q_j is sufficiently small. This will help us remove those local extrema in $\mu''_\gamma(t)$ generated from the detected Type II change points in the previous step and hence to detect the Type I change points via detecting peaks in $\mu''_\gamma(t)$ by Proposition 1 (see Step 2 in Algorithm 3).

Remark 2. A Type II change point v_j with large $|q_j|$ behaves similarly to a Type I change point, its derivatives exhibit similar characteristics (see Figure 2 below). Specifically, a Type II change point with q_j large enough such that $q_j > c/\gamma$ can not generate a local extremum in the first derivative $\mu'_\gamma(t)$; and the corresponding second derivative $\mu''_\gamma(t)$ has only one local extremum around the change point v_j . Since $a_j \neq 0$ and $q_j > c/\gamma$, one has $v_j + \gamma^2 q_j > v_j + c\gamma$, implying no local extremum in the first derivative $\mu'_\gamma(t)$ (see (6a)). Additionally,

$$v_j + \frac{1}{2} \left(\gamma^2 q_j + \gamma \sqrt{\gamma^2 q_j^2 + 4} \right) > v_j + c\gamma, \quad v_j + \frac{1}{2} \left(\gamma^2 q_j - \gamma \sqrt{\gamma^2 q_j^2 + 4} \right) \approx v_j. \quad (8)$$

Hence there is only one local extremum around v_j in the second derivative $\mu''_\gamma(t)$ (see (7a)). Given this behavior, it is reasonable to interpret a Type II change point with large $|q_j|$ as a special case that

essentially behaves like Type I change points ($q_j = \infty$ as $a_j = 0$).

Intuitively, for a Type II change point v_j , if the $|q_j|$ is large enough such that $q_j > c/\gamma$, it means the slope change dominates the jump size, thereafter this Type II change point behaves similarly to a Type I change point. In this paper, we do not consider the case of large $|q_j|$. However, as discussed above, this case can be essentially treated as the case of Type I change points.

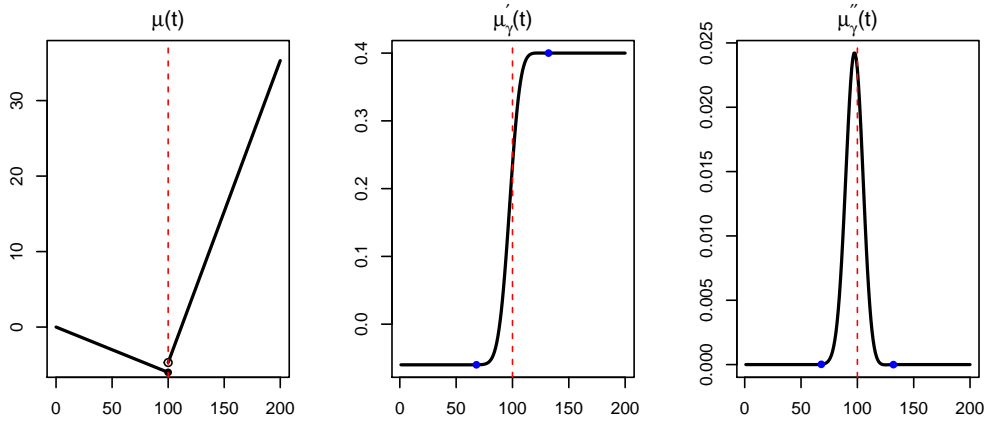


Figure 2: Characteristics of the Type II change point v_j with large $|q_j|$. In the left plot of signal $\mu(t)$, the slope change dominates the jump size, giving a large $|q_j|$. The middle plot of the first derivative μ'_γ shows no local extremum, and the right plot of the second derivative $\mu''_\gamma(t)$ shows a local maximum around the change point v_j . This special Type II change point can be essentially treated as a Type I change point.

2.3 Main ideas

Figure 1 demonstrates the key concept of the proposed change point detection method. The main idea is to transform the problem of change point detection in a data sequence into testing local extrema in the derivatives of the smoothed signal. A candidate peak can arise either from a true change point in the signal region or from pure random noise. Multiple testing based on the peak height distribution of the first and second derivatives is then employed to identify the significant

peaks as the true change points. Notice that, although this main idea (or Figure 1) is illustrated over signal $\mu(t)$, it is also applicable to the signal-plus-noise $y(t)$ under certain asymptotic conditions such that the signal strength (size of jump or slope change) and length of data sequence are large; see conditions (C1) and (C2) below.

To further illustrate the main idea, especially the proposed algorithm, toy examples are presented in Figures 3 and 4. In Scenario 1 (pure Type I change points), a Type I change point generates a peak exactly at its location in the second derivative $\mu''_\gamma(t)$, as indicated in (7b). In Scenario 2 (pure Type II change points), a Type II change point produces a peak in the first derivative $\mu'_\gamma(t)$ around its location, as described in (6a). By subtracting the corresponding baseline (piecewise slope at v_j) from the peaks in $y'_\gamma(t)$, the problem reduces to a standard peak detection problem. In Scenario 3, a combination of Type I and Type II change points is considered. The Type II change points are first identified based on the peaks in $y'_\gamma(t)$, and then the Type I change points are detected as significant peaks in $y''_\gamma(t)$ after cutting off the Type II change points.

Our proposed method, called **mSTEM** (**m**odified **S**moothering and **T**esting of **M**axima/**M**inima), consists of the following steps and provides a framework for change point detection.

1. Differential kernel smoothing: to transform change points into local maxima or minima (illustrated in Figure 1), and can meanwhile increase the signal-noise-ratio (SNR).
2. Candidate peaks: to find local extrema of either the first or second derivative of the smoothed observed data.
3. P-values: to compute the p-value of each local maximum or minimum under the null hypothesis of no change point (no signal) in a local neighborhood.
4. Multiple testing: to apply a multiple testing procedure (Benjamini-Hochberg procedure) to the set of local maxima and minima; a change point is claimed to be detected if the p-value is significant.

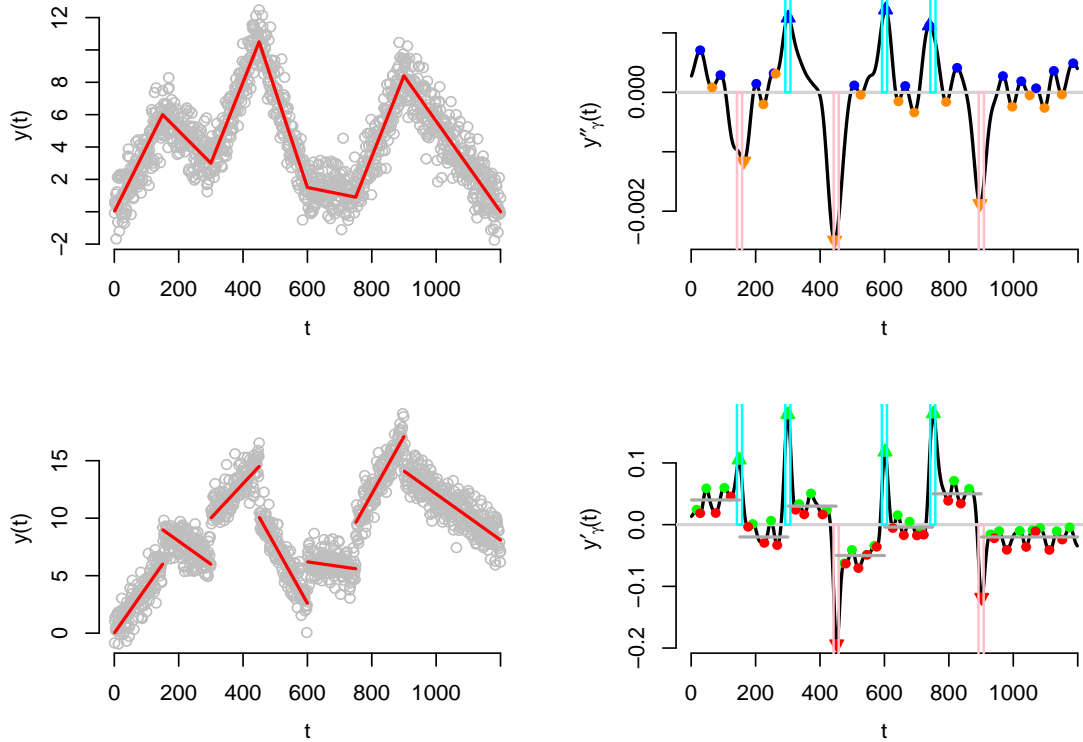


Figure 3: Process of Type I and Type II change point detection. The two plots on the left panel show the data (grey circles) with six Type I change points and the data with six Type II change points respectively. Here, the red lines indicate piecewise linear signals $\mu(t)$. The two plots (black lines) on the right panels show the second and first derivatives of the smoothed data respectively obtained from convolving data with the Gaussian kernel with bandwidth $\gamma = 8$. In the first derivative $y'_\gamma(t)$, local maxima and local minima are represented by green and red dots respectively. In the second derivative $y''_\gamma(t)$, they are represented by blue and orange dots respectively. The triangles indicate the significant local extrema under significant level $\alpha = 0.05$. The cyan and pink bars show the location tolerance intervals $(v_j - b, v_j + b)$ with $b = 5$ for the true increasing and decreasing change points respectively. The grey horizontal lines (lower right plot) indicate piecewise slopes of the signal, serving as baselines in the testing of $y'_\gamma(t)$. In these two testings, all change points of both Type I and Type II are detected perfectly without any false discovery.

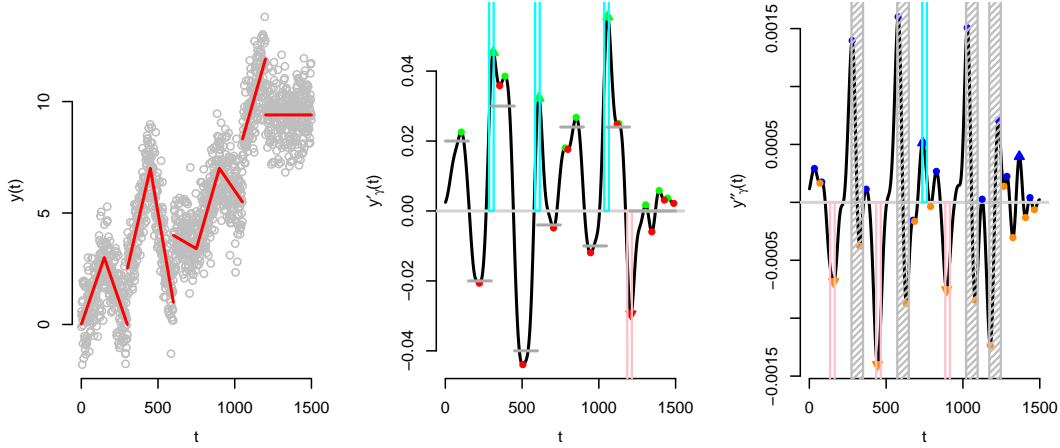


Figure 4: Process of mixture of Type I and Type II change point detection. The same graphical symbols and colors as in Figure 3 are utilized here. The left plot (grey circles) shows the data with four Type I and four Type II change points. The middle plot shows the first derivative of the smoothed data $y'_\gamma(t)$ for detection of Type II change points. The right plot shows the second derivative of the smoothed data $y''_\gamma(t)$. The Type II change points are first detected in the first derivative $y'_\gamma(t)$ (the middle plot). Then the local extrema in the second derivative $y''_\gamma(t)$ generated by the detected Type II change points are removed (represented by grey shaded bars and each bar is $[v_j - 2\gamma, v_j + 2\gamma]$). After this filtering process, the remaining significant local extrema in $y''_\gamma(t)$ are identified as Type I change points. In this testing, all Type I and Type II change points are detected without any false discovery.

3 Multiple change point detection for linear models

Suppose we observed $y(t)$ defined by (1) with J change points in the line of length L centered at the origin, which is denoted by $U(L) = (-L/2, L/2)$. We define the *signal region* as $\mathbb{S}_1 = \cup_{j=1}^J S_j = \cup_{j=1}^J (v_j - b, v_j + b)$, which is the region of interest where the true change points are expected to occur. It is defined as the union of intervals centered around each true change point v_j . The *null region* is the complement of the signal region within $U(L)$ given by $\mathbb{S}_0 = U(L) \setminus \mathbb{S}_1$, where no true change points are expected to occur.

3.1 Pure Type I change point detection

We consider first the case of pure Type I change points, which do not generate any peak in $\mu'_\gamma(t)$ by (6b). Applying Proposition 1, it is appropriate to detect the Type I change points via detecting peaks in $y''_\gamma(t)$. Following the proposed mSTEM procedure of change point detection in Section 2.3, we give below the mSTEM algorithm for the detection of Type I change points.

Algorithm 1 (mSTEM algorithm for Type I change point detection).

1. Differential kernel smoothing: Obtain the process $y''_\gamma(t)$ in (5) by convolution of $y(t)$ with the kernel derivative $w''_\gamma(t)$.
2. Candidate peaks: Find the set of local maxima and minima of $y''_\gamma(t)$ in $U(L)$, denoted by $\tilde{T}_1 = \tilde{T}_1^+ \cup \tilde{T}_1^-$, where

$$\tilde{T}_1^+ = \left\{ t \in U(L) : y_\gamma^{(3)}(t) = 0, y_\gamma^{(4)}(t) < 0 \right\},$$

$$\tilde{T}_1^- = \left\{ t \in U(L) : y_\gamma^{(3)}(t) = 0, y_\gamma^{(4)}(t) > 0 \right\}.$$

Note that \tilde{T}_1^+ and \tilde{T}_1^- are the sets of local maxima and minima in $y''_\gamma(t)$, respectively.

3. P-values: For each $t \in \tilde{T}_1^+$, compute the p-value $p_1(t)$ for testing the hypotheses

$$\mathcal{H}_0(t) : \{ \mu''(s) = 0 \text{ for all } s \in (t - b, t + b) \} \quad \text{vs.}$$

$$\mathcal{H}_A(t) : \{ \mu'(s+) > \mu'(s-) \text{ for some } s \in (t - b, t + b) \};$$

and for each $t \in \tilde{T}_1^-$, compute the p -value $p_I(t)$ for testing the hypotheses

$$\mathcal{H}_0(t) : \{\mu''(s) = 0 \text{ for all } s \in (t - b, t + b)\} \text{ vs.}$$

$$\mathcal{H}_A(t) : \{\mu'(s+) < \mu'(s-) \text{ for some } s \in (t - b, t + b)\},$$

where $\mu'(s+) = \lim_{x \rightarrow s+} \mu'(x)$, $\mu'(s-) = \lim_{x \rightarrow s-} \mu'(x)$ and $b > 0$ is an appropriate location tolerance parameter.

4. Multiple testing: Apply the Benjamini-Hochberg (BH) multiple testing procedure on the set of p -values $\{p_I(t), t \in \tilde{T}_1\}$, defined in Section 3.1.1 below, and declare all significant local extrema whose p -values are smaller than the significance threshold.

3.1.1 P-value calculation

The p -value in step 3 of Algorithm 1 is given by

$$p_I(t) = \begin{cases} F_{z''_\gamma}(y''_\gamma(t)) & t \in \tilde{T}_1^+, \\ F_{z''_\gamma}(-y''_\gamma(t)) & t \in \tilde{T}_1^-, \end{cases} \quad (9)$$

where $F_{z''_\gamma}(u)$ (defined in Section 3.4 below) is the right tail probability of $z''_\gamma(t)$ at the local maximum $t \in \tilde{T}_1^+$, evaluated under the null model $\mu''_\gamma(s) = 0, \forall s \in (t - b, t + b)$, i.e.,

$$F_{z''_\gamma}(u) = P(z''_\gamma(t) > u \mid t \text{ is a local maximum of } z''_\gamma(t)). \quad (10)$$

The second line in (9) is obtained by the following symmetry property and the fact that z''_γ and $-z''_\gamma$ have the same distribution,

$$\begin{aligned} & P(z''_\gamma(t) < u \mid t \text{ is a local minimum of } z''_\gamma(t)) \\ &= P(-z''_\gamma(t) > -u \mid t \text{ is a local maximum of } -z''_\gamma(t)) = F_{z''_\gamma}(-u). \end{aligned}$$

3.1.2 Error and power definitions

For $u > 0$, we define $\tilde{T}_1(u) = \tilde{T}_1^+(u) \cup \tilde{T}_1^-(u)$, where

$$\begin{aligned}\tilde{T}_1^+(u) &= \left\{ t \in U(L) : y_\gamma''(t) > u, y_\gamma^{(3)}(t) = 0, y_\gamma^{(4)}(t) < 0 \right\}, \\ \tilde{T}_1^-(u) &= \left\{ t \in U(L) : y_\gamma''(t) < -u, y_\gamma^{(3)}(t) = 0, y_\gamma^{(4)}(t) > 0 \right\}.\end{aligned}$$

It is seen that $\tilde{T}_1^+(u)$ and $\tilde{T}_1^-(u)$ are respectively the set of local maxima of $y_\gamma''(t)$ above u and the set of local minima of $y_\gamma''(t)$ below $-u$. The number of totally and falsely detected change points at threshold u are defined respectively as

$$R_1(u) = \#\{t \in \tilde{T}_1(u)\}, \quad V_1(u) = \#\{t \in \tilde{T}_1(u) \cap \mathbb{S}_0\}. \quad (11)$$

Both are defined as zero if $\tilde{T}_1(u)$ is empty. The FDR at threshold u is defined as the expected proportion of falsely detected change points

$$\text{FDR}_1(u) = \text{E} \left\{ \frac{V_1(u)}{R_1(u) \vee 1} \right\}. \quad (12)$$

Denote by \mathcal{I}_1^+ and \mathcal{I}_1^- the collections of indices j corresponding to increasing and decreasing (in slope change) Type I change points respectively. The power is defined as

$$\begin{aligned}\text{Power}_1(u) &= \frac{1}{J} \sum_{j=1}^J P \left(\tilde{T}_1(u) \cap S_j \neq \emptyset \right) \\ &= \frac{1}{J} \left[\sum_{j \in \mathcal{I}_1^+} P \left(\tilde{T}_1^+(u) \cap S_j \neq \emptyset \right) + \sum_{j \in \mathcal{I}_1^-} P \left(\tilde{T}_1^-(u) \cap S_j \neq \emptyset \right) \right],\end{aligned} \quad (13)$$

where each $P(\cdot)$ is the probability of detecting change point v_j within the signal region $S_j = (v_j - b, v_j + b)$. Throughout this paper, when considering local extrema of the second derivative of the process over the signal region S_j or the smoothed signal region $S_{j,\gamma} = (v_j - c\gamma, v_j + c\gamma)$ around j , the local extrema are regarded as local maxima if $j \in \mathcal{I}_1^+$ and as local minima if $j \in \mathcal{I}_1^-$, respectively.

3.1.3 Asymptotic FDR control and power consistency

Denote by $E[\tilde{m}_{z''_\gamma}(U(1))]$ and $E[\tilde{m}_{z''_\gamma}(U(1), u)]$ the expected number of local extrema, and the expected number of both local maxima above level u and local minima below $-u$ of $z''_\gamma(t)$ on the unit interval $U(1) = (-1/2, 1/2)$, respectively. Note that, by symmetry, the expected number of local minima of $z''_\gamma(t)$ below level $-u$ equals the expected number of local maxima of $z''_\gamma(t)$ above u , which is $E[\tilde{m}_{z''_\gamma}(U(1), u)]/2$. Similarly, we define accordingly $E[\tilde{m}_{z'_\gamma}(U(1))]$ and $E[\tilde{m}_{z'_\gamma}(U(1), u)]$ for $z'_\gamma(t)$ on $U(1)$.

Recall that the BH procedure applied in step 4 of Algorithm 1 is defined as follows. Let m_I be the size of the set \tilde{T}_I . For a fixed $\alpha \in (0, 1)$, let ℓ be the largest index for which the i th smallest p-value is less than $i\alpha/m_I$. Then the null hypothesis $\mathcal{H}_0(t)$ at $t \in \tilde{T}_I$ is rejected if

$$p_I(t) < \frac{\ell\alpha}{m_I} \iff \begin{cases} y''_\gamma(t) > \tilde{u}_I = F_{z''_\gamma}^{-1}\left(\frac{\ell\alpha}{m_I}\right) & \text{if } t \in \tilde{T}_I^+, \\ y''_\gamma(t) < -\tilde{u}_I = -F_{z''_\gamma}^{-1}\left(\frac{\ell\alpha}{m_I}\right) & \text{if } t \in \tilde{T}_I^-, \end{cases} \quad (14)$$

where $\ell\alpha/m_I$ is defined as 1 if $m_I = 0$. Note that \tilde{T}_I and hence m_I and \tilde{u}_I are also random, which are different from the usual BH procedure. We define the FDR in such BH procedure as

$$\text{FDR}_{I,\text{BH}} = E \left\{ \frac{V_I(\tilde{u}_I)}{R_I(\tilde{u}_I) \vee 1} \right\}, \quad (15)$$

where $R_I(\cdot)$ and $V_I(\cdot)$ are defined in (11) and the expectation is taken over all possible realizations of the random threshold \tilde{u}_I . Similarly, the corresponding power, denoted by $\text{Power}_{I,\text{BH}}$, is defined as (13) with u replaced by \tilde{u}_I .

For the asymptotic theories of Type I change point detection, we make the assumption:

$$(C1) \quad L \rightarrow \infty, k = \inf_j |k_{j+1} - k_j| \rightarrow \infty \text{ and } k^2/\log L \rightarrow \infty.$$

Theorem 1. *Suppose that $y(t)$ contains only Type I change points, the condition (C1) holds and $J/L \rightarrow A > 0$ as $L \rightarrow \infty$.*

(i) If Algorithm 1 is applied with a fixed threshold u , then

$$\text{FDR}_I(u) \rightarrow \frac{E[\tilde{m}_{z''_\gamma}(U(1), u)](1 - 2c\gamma A)}{E[\tilde{m}_{z''_\gamma}(U(1), u)](1 - 2c\gamma A) + A}, \quad (16)$$

$$\text{Power}_I(u) \rightarrow 1. \quad (17)$$

(ii) If Algorithm 1 is applied with the random threshold \tilde{u}_I , then

$$\text{FDR}_{I,\text{BH}} \rightarrow \alpha \frac{E[\tilde{m}_{z''_\gamma}(U(1))](1 - 2c\gamma A)}{E[\tilde{m}_{z''_\gamma}(U(1))](1 - 2c\gamma A) + A}, \quad (18)$$

$$\text{Power}_{I,\text{BH}} \rightarrow 1. \quad (19)$$

Note that, by the definition of d , we have $Jd < L$ or $d < L/J \rightarrow 1/A$. Meanwhile, it is assumed $d = \inf_j(v_j - v_{j-1}) > 2c\gamma$, thus we have $1/A > 2c\gamma$ and hence $1 - 2c\gamma A > 0$.

3.2 Pure Type II change point detection

In the detection of Type I breaks, by taking the second derivative, the piecewise linear parts of $\mu(t)$ become 0 in $\mu''_\gamma(t)$ over $\mathbb{R} \setminus \mathbb{S}_{1,\gamma}$, where $\mathbb{S}_{1,\gamma} = \cup_{j=1}^J (v_j - c\gamma, v_j + c\gamma)$ is the *smoothed signal region* (see the intervals indicated by the blue points in Figure 1). However, in the detection of Type II breaks, the piecewise linear parts become piecewise constants (the slopes) in $\mu'_\gamma(t)$ over $\mathbb{R} \setminus \mathbb{S}_{1,\gamma}$. To detect Type II breaks, the null hypothesis (no signal/jump) $\mu'_\gamma(t) = k(t)$, where $k(t)$ is the corresponding piecewise slope at t , will be tested. Hence, it is crucial to estimate the piecewise slopes around the change points v_j .

3.2.1 Piecewise slopes estimate

The main idea of estimation of piecewise slopes is to divide the data sequence into segments and estimate the slopes within each segment using linear regression. These segments are determined based on the presence of pairwise local maxima and minima, which are located near $v_j \pm \gamma$ around change points in the second derivative $\mu''_\gamma(t)$ (see Figure 1 (f)).

To ensure that all true Type II breaks are captured and to give a better estimate of the piecewise slopes, Algorithm 1 is applied with a larger significance level, such as 0.1. This helps in obtaining non-conservative initial estimators for Type II change points based on the peaks detected in $y'_\gamma(t)$. Then within each segment the piecewise slope is estimated using a robust regression model (Huber, 2004) to mitigate the disturbance of change points.

Once the piecewise slopes are obtained, we will apply the following algorithm, which is based on local extrema of the first derivative of the smoothed data, to detect Type II change points.

Algorithm 2 (mSTEM algorithm for Type II change point detection).

1. Differential kernel smoothing: Obtain the process $y'_\gamma(t)$ in (5) by convolution of $y(t)$ with the kernel derivative $w'_\gamma(t)$.

2. Candidate peaks: Find the set of local maxima and minima of $y'_\gamma(t)$ in $U(L)$, denoted by $\tilde{T}_\Pi = \tilde{T}_\Pi^+ \cup \tilde{T}_\Pi^-$, where

$$\begin{aligned}\tilde{T}_\Pi^+ &= \left\{ t \in U(L) : y''_\gamma(t) = 0, y_\gamma^{(3)}(t) < 0 \right\}, \\ \tilde{T}_\Pi^- &= \left\{ t \in U(L) : y''_\gamma(t) = 0, y_\gamma^{(3)}(t) > 0 \right\}.\end{aligned}$$

3. P-values: For each $t \in \tilde{T}_\Pi^+$, compute the p-value $p_\Pi(t)$ for testing the hypotheses

$$\mathcal{H}_0(t) : \{ \mu'(s) = k(s) \text{ for all } s \in (t - b, t + b) \} \quad \text{vs.}$$

$$\mathcal{H}_A(t) : \{ \mu(s+) > \mu(s-) \text{ for some } s \in (t - b, t + b) \},$$

where $k(s)$ is the piecewise slope at s , $\mu(s+) = \lim_{x \rightarrow s+} \mu(x)$, $\mu(s-) = \lim_{x \rightarrow s-} \mu(x)$ and $b > 0$ is an appropriate location tolerance parameter. For each $t \in \tilde{T}_\Pi^-$, compute the p-value $p_\Pi(t)$ for testing the hypotheses

$$\mathcal{H}_0(t) : \{ \mu'(s) = k(s) \text{ for all } s \in (t - b, t + b) \} \quad \text{vs.}$$

$$\mathcal{H}_A(t) : \{ \mu(s+) < \mu(s-) \text{ for some } s \in (t - b, t + b) \}.$$

4. Multiple testing: Apply the BH multiple testing procedure on the set of p-values $\{p_\Pi(t), t \in \tilde{T}_\Pi\}$, and declare significant all local extrema whose p-values are smaller than the significance threshold.

Similarly to (9) and (10), the p-value in step 3 of Algorithm 2 is given by

$$p_{\Pi}(t) = \begin{cases} F_{z'_\gamma}(y'_\gamma(t) - k(t)) & t \in \tilde{T}_{\Pi}^+, \\ F_{z'_\gamma}(-(y'_\gamma(t) - k(t))) & t \in \tilde{T}_{\Pi}^-. \end{cases}$$

Here $F_{z'_\gamma}(u)$ is the right tail probability of $z'_\gamma(t)$ at the local maximum $t \in \tilde{T}_{\Pi}^+$, as defined in Section 3.4 below, which is

$$F_{z'_\gamma}(u) = P(z'_\gamma(t) > u \mid t \text{ is a local maximum of } z'_\gamma(t)).$$

3.2.2 Error and power definitions

For $u > 0$, we define $\tilde{T}_{\Pi}(u) = \tilde{T}_{\Pi}^+(u) \cup \tilde{T}_{\Pi}^-(u)$, where

$$\begin{aligned} \tilde{T}_{\Pi}^+(u) &= \left\{ t \in U(L) : y'_\gamma(t) - k(t) > u, y''_\gamma(t) = 0, y_\gamma^{(3)}(t) < 0 \right\}, \\ \tilde{T}_{\Pi}^-(u) &= \left\{ t \in U(L) : y'_\gamma(t) - k(t) < -u, y''_\gamma(t) = 0, y_\gamma^{(3)}(t) > 0 \right\}. \end{aligned}$$

The number of totally and falsely detected change points and the FDR at threshold u are defined respectively as

$$R_{\Pi}(u) = \#\{t \in \tilde{T}_{\Pi}(u)\}, \quad V_{\Pi}(u) = \#\{t \in \tilde{T}_{\Pi}(u) \cap \mathcal{S}_0\}, \quad \text{FDR}_{\Pi}(u) = \mathbb{E} \left\{ \frac{V_{\Pi}(u)}{R_{\Pi}(u) \vee 1} \right\}. \quad (20)$$

Denote by \mathcal{I}_{Π}^+ and \mathcal{I}_{Π}^- the sets of indices j corresponding to increasing and decreasing (in jump)

Type II change points v_j , respectively. The power is defined as

$$\begin{aligned} \text{Power}_{\Pi}(u) &= \frac{1}{J} \sum_{j=1}^J P(\tilde{T}_{\Pi}(u) \cap S_j \neq \emptyset) \\ &= \frac{1}{J} \left[\sum_{j \in \mathcal{I}_{\Pi}^+} P(\tilde{T}_{\Pi}^+(u) \cap S_j \neq \emptyset) + \sum_{j \in \mathcal{I}_{\Pi}^-} P(\tilde{T}_{\Pi}^-(u) \cap S_j \neq \emptyset) \right]. \end{aligned} \quad (21)$$

Throughout this paper, when considering local extrema over the signal region $S_j = (v_j - b, v_j + b)$ or the smoothed signal region $S_{j,\gamma} = (v_j - c\gamma, v_j + c\gamma)$ around j , the local extrema of the derivative of the process are regarded as local maxima if $j \in \mathcal{I}_{\Pi}^+$ and as local minima if $j \in \mathcal{I}_{\Pi}^-$, respectively.

3.2.3 Asymptotic FDR control and power consistency

Suppose the BH procedure is applied in step 4 of Algorithm 2 as follows. Define m_{II} as the size of set \tilde{T}_{II} . For a fixed $\alpha \in (0, 1)$, let ℓ be the largest index for which the i th smallest p-value is less than $i\alpha/m_{\text{II}}$. Then the null hypothesis $\mathcal{H}_0(t)$ at $t \in \tilde{T}_{\text{II}}$ is rejected if

$$p_{\text{II}}(t) < \frac{\ell\alpha}{m_{\text{II}}} \iff \begin{cases} y'_\gamma(t) - k(t) > \tilde{u}_{\text{II}} = F_{z'_\gamma}^{-1}\left(\frac{\ell\alpha}{m_{\text{II}}}\right) & \text{if } t \in \tilde{T}_{\text{II}}^+, \\ y'_\gamma(t) - k(t) < -\tilde{u}_{\text{II}} = -F_{z'_\gamma}^{-1}\left(\frac{\ell\alpha}{m_{\text{II}}}\right) & \text{if } t \in \tilde{T}_{\text{II}}^-, \end{cases} \quad (22)$$

where $F_{z'_\gamma}$ is defined in (10) with z''_γ replaced by z'_γ , and $\ell\alpha/m_{\text{II}}$ is defined as 1 if $m_{\text{II}} = 0$. Since \tilde{u}_{II} is random, we define FDR in such BH procedure as

$$\text{FDR}_{\text{II,BH}} = E \left\{ \frac{V_{\text{II}}(\tilde{u}_{\text{II}})}{R_{\text{II}}(\tilde{u}_{\text{II}}) \vee 1} \right\},$$

where $R_{\text{II}}(\cdot)$ and $V_{\text{II}}(\cdot)$ are defined in (20) and the expectation is taken over all possible realizations of the random threshold \tilde{u}_{II} . Similarly, the corresponding power, denoted by $\text{Power}_{\text{II,BH}}$, is defined as (13) with u replaced by \tilde{u}_{II} .

To establish asymptotic theories for Type II change point detection, we make the assumption:

$$(C2) \quad a = \inf_j |a_j| \rightarrow \infty, \quad q = \sup_j \left| \frac{k_{j+1} - k_j}{a_j} \right| \rightarrow 0 \quad \text{and} \quad \frac{\log L}{a^2} \rightarrow 0 \quad \text{as } L \rightarrow \infty.$$

Theorem 2. *Suppose $y(t)$ contains only Type II change points, the condition (C2) holds and $J/L \rightarrow A > 0$ as $L \rightarrow \infty$.*

(i) *If Algorithm 2 is applied with a fixed threshold u , then*

$$\text{FDR}_{\text{II}}(u) \rightarrow \frac{E[\tilde{m}_{z'_\gamma}(U(1), u)](1 - 2c\gamma A)}{E[\tilde{m}_{z'_\gamma}(U(1), u)](1 - 2c\gamma A) + A} \quad \text{and} \quad \text{Power}_{\text{II}}(u) \rightarrow 1.$$

(ii) *If Algorithm 2 is applied with random threshold \tilde{u}_{II} , then*

$$\text{FDR}_{\text{II,BH}} \rightarrow \alpha \frac{E[\tilde{m}_{z'_\gamma}(U(1))](1 - 2c\gamma A)}{E[\tilde{m}_{z'_\gamma}(U(1))](1 - 2c\gamma A) + A} \quad \text{and} \quad \text{Power}_{\text{II,BH}} \rightarrow 1.$$

3.3 Mixture of Type I and Type II change point detection

We have shown that pure Type I and Type II change points can be detected through peak detection in the second derivative $y''_\gamma(t)$ (see Algorithm 1) and the first derivative $y'_\gamma(t)$ (see Algorithm 2), respectively. However, it is very common that a real signal contains both Type I and Type II change points. Distinguishing between Type I and Type II change points is a key challenge when managing signals comprising a combination of these types. Our strategy involves initially identifying Type II change points via peak detection within the first derivative $y'_\gamma(t)$, and then detect Type I change points by excluding the locations of Type II change points from consideration in the second derivative $y''_\gamma(t)$. The rationale behind this approach is as follows:

1. Type II change points generate peaks in the first derivative $y'_\gamma(t)$, while Type I change points do not. By detecting significant peaks in $y'_\gamma(t)$ using Algorithm 2, we can identify the locations of Type II change points.
2. Once the Type II change points are identified, we can focus on detecting Type I change points. Note that both Type I and Type II change points can produce peaks in the second derivative $y''_\gamma(t)$. However, some of these peaks may be generated by Type II change points, and we want to exclude them from our Type I detection.

To distinguish between Type I and Type II change points in the mixture case, we remove the Type II change points detected in the first step from consideration. This means that any peaks in the second derivative $y''_\gamma(t)$ that coincide with the locations of Type II change points are excluded from the set of potential Type I change points. The remaining peaks in $y''_\gamma(t)$, which are not associated with Type II change points, are more likely to be generated by Type I change points.

Algorithm 3 (mSTEM algorithm for mixture of Type I and II change point detection).

1. Detect Type II breaks: *Perform Algorithm 2 to obtain estimates of Type II breaks, denoted as $\hat{v}_i \in \tilde{T}_{\text{II}}$ for $i = 1, \dots, R_{\text{II}}$. A larger γ in this step is suggested to have a better estimate*

of Type II change points and less false discoveries. Because a larger γ generally results in a higher SNR (Signal-to-Noise ratio, see Section 3.5).

2. Candidate Type I peaks: Find the set of local maxima and minima of $y''_\gamma(t)$ in $U(L)$, denoted by $\tilde{T}_I = \tilde{T}_I^+ \cup \tilde{T}_I^-$. As \tilde{T}_I contains local extrema generated by both Type I and Type II breaks, it is necessary to remove the peaks generated by Type II breaks which are detected in step 1. Let $\mathbb{S}_{II}^* = \cup_{i=1}^{R_{II}} (\hat{v}_i - 2\gamma, \hat{v}_i + 2\gamma)$ be the removed region, then the set of candidate peaks of Type I breaks is defined as $\tilde{T}_{I \setminus II} = \tilde{T}_{I \setminus II}^+ \cup \tilde{T}_{I \setminus II}^-$, where

$$\tilde{T}_{I \setminus II}^+ = \tilde{T}_I^+ \setminus \mathbb{S}_{II}^*, \quad \tilde{T}_{I \setminus II}^- = \tilde{T}_I^- \setminus \mathbb{S}_{II}^*.$$

3. P-values: For each $t \in \tilde{T}_{I \setminus II}^+$, compute the p-value $p_{I \setminus II}(t)$ for testing the hypotheses

$$\mathcal{H}_0(t) : \{\mu''(s) = 0 \text{ for all } s \in (t - b, t + b)\} \text{ vs.}$$

$$\mathcal{H}_A(t) : \{\mu'(s+) > \mu'(s-) \text{ for some } s \in (t - b, t + b)\};$$

and for each $t \in \tilde{T}_{I \setminus II}^-$, compute the p-value $p_I(t)$ for testing the hypotheses

$$\mathcal{H}_0(t) : \{\mu''(s) = 0 \text{ for all } s \in (t - b, t + b)\} \text{ vs.}$$

$$\mathcal{H}_A(t) : \{\mu'(s+) < \mu'(s-) \text{ for some } s \in (t - b, t + b)\}.$$

4. Multiple testing: Apply a multiple testing procedure on the set of p-values $\{p_{I \setminus II}(t), t \in \tilde{T}_{I \setminus II}\}$, and declare significant all local extrema whose p-values are smaller than the significance threshold.

3.3.1 Asymptotic FDR control and power consistency

Let $\mathbb{S}_{1, I \setminus II} = \cup_{j=1}^{J_1} (v_j - b, v_j + b) \setminus \mathbb{S}_{II}^*$ be the signal region of Type I change points, and $\mathbb{S}_{0, I \setminus II} = U(L) \setminus \mathbb{S}_{1, I \setminus II}$ be the null region of Type I change points. Then the number of totally and falsely detected Type I change points at threshold u are defined respectively as

$$R_{I \setminus II}(u) = \#\{t \in \tilde{T}_{I \setminus II}(u)\}, \quad V_{I \setminus II}(u) = \#\{t \in \tilde{T}_{I \setminus II}(u) \cap \mathbb{S}_{0, I \setminus II}\}. \quad (23)$$

Given fixed thresholds u_1 and u_2 for Type I and Type II change point detection respectively, FDR is defined as

$$\text{FDR}_{\text{III}}(u_1, u_2) = \mathbb{E} \left\{ \frac{V_{\text{I}\setminus\text{II}}(u_1) + V_{\text{II}}(u_2)}{[R_{\text{I}\setminus\text{II}}(u_1) + R_{\text{II}}(u_2)] \vee 1} \right\},$$

and the power is defined as

$$\begin{aligned} & \text{Power}_{\text{III}}(u_1, u_2) \\ &= \frac{1}{J} \left[\sum_{j \in \mathcal{I}_1^+} P \left(\tilde{T}_{\text{I}\setminus\text{II}}^+(u_1) \cap (v_j - b, v_j + b) \neq \emptyset \right) + \sum_{j \in \mathcal{I}_1^-} P \left(\tilde{T}_{\text{I}\setminus\text{II}}^-(u_1) \cap (v_j - b, v_j + b) \neq \emptyset \right) \right. \\ & \quad \left. + \sum_{j \in \mathcal{I}_2^+} P \left(\tilde{T}_{\text{II}}^+(u_2) \cap (v_j - b, v_j + b) \neq \emptyset \right) + \sum_{j \in \mathcal{I}_2^-} P \left(\tilde{T}_{\text{II}}^-(u_2) \cap (v_j - b, v_j + b) \neq \emptyset \right) \right]. \end{aligned} \quad (24)$$

For random thresholds \tilde{u}_1 and \tilde{u}_2 defined in (14) and (22) respectively, the FDR is

$$\text{FDR}_{\text{III,BH}} = \mathbb{E} \left\{ \frac{V_{\text{I}\setminus\text{II}}(\tilde{u}_1) + V_{\text{II}}(\tilde{u}_2)}{[R_{\text{I}\setminus\text{II}}(\tilde{u}_1) + R_{\text{II}}(\tilde{u}_2)] \vee 1} \right\}.$$

Similarly, the corresponding power, denoted by $\text{Power}_{\text{III,BH}}$, is defined as (24) with u_1 and u_2 replaced by \tilde{u}_1 and \tilde{u}_2 respectively.

Theorem 3. *Suppose $y(t)$ contains J_1 Type I change points and J_2 Type II change points ($J = J_1 + J_2$), conditions (C1) and (C2) hold, and $J_1/L \rightarrow A_1 > 0$ and $J_2/L \rightarrow A_2 > 0$ as $L \rightarrow \infty$.*

(i) *If Algorithm 3 is applied with fixed thresholds u_1 and u_2 for Type I and Type II change points respectively, then*

$$\limsup \text{FDR}_{\text{III}}(u_1, u_2) \leq \frac{E[\tilde{m}_{z_\gamma'}(U(1), u_1)](1 - 2c\gamma A_1) + E[\tilde{m}_{z_\gamma'}(U(1), u_2)](1 - 2c\gamma A_2)}{E[\tilde{m}_{z_\gamma'}(U(1), u_1)](1 - 2c\gamma A_1) + E[\tilde{m}_{z_\gamma'}(U(1), u_2)](1 - 2c\gamma A_2) + A}, \quad (25)$$

$$\text{Power}_{\text{III}}(u_1, u_2) \rightarrow 1. \quad (26)$$

(ii) *If Algorithm 3 is applied with random thresholds \tilde{u}_1 and \tilde{u}_2 for Type I and Type II change*

points respectively, then

$$\limsup \text{FDR}_{\text{III,BH}} \leq \alpha, \quad (27)$$

$$\text{Power}_{\text{III,BH}} \rightarrow 1. \quad (28)$$

3.4 Gaussian auto-correlation models and related peak height distributions

Let $X(t)$ be a centered smooth stationary Gaussian process with variance σ^2 . Note that, due to the stationarity, $E(X(t)X''(t)) = -\text{Var}(X'(t))$. Define

$$\eta = -\text{Corr}(X(t), X''(t)) = \frac{\text{Var}(X'(t))}{\sqrt{\text{Var}(X(t))\text{Var}(X''(t))}}.$$

Let $F_X(x)$ denote the right tail probability of $X(t)$ conditional on t being a local maximum, then

$$\begin{aligned} F_X(x) &= P(X(t) > x \mid t \text{ is a local maximum of } X) \\ &= 1 - \Phi\left(\frac{x}{\sigma\sqrt{1-\eta^2}}\right) + \sqrt{2\pi}\eta\phi\left(\frac{x}{\sigma}\right)\Phi\left(\frac{\eta x}{\sigma\sqrt{1-\eta^2}}\right). \end{aligned} \quad (29)$$

Note that (29) is a general version of the peak height distribution derived in [Schwartzman et al. \(2011\)](#) and [Cheng and Schwartzman \(2015\)](#). One important and appealing characteristic of (29) is that, for a unit-variance process, it only depends on a single parameter η , the negative correlation between the process and its second derivative.

To implement the simulations below, we consider here a specific example of $X(t)$ and derive the peak height distributions. Let the noise $z(t)$ be

$$z(t) = \int_{\mathbb{R}} \frac{1}{\nu} \phi\left(\frac{t-s}{\nu}\right) dB(s), \quad \nu > 0, \quad (30)$$

where $dB(s)$ is Gaussian white noise ($z(t)$ is regarded by convention as Gaussian white noise when $\nu = 0$). Convolution with a Gaussian kernel $w_\gamma(t) = (1/\gamma)\phi(t/\gamma)$ with $\gamma > 0$ produces a zero-mean infinitely differentiable stationary Gaussian process

$$z_\gamma(t) = \int_{\mathbb{R}} w_\gamma(t-x)z(x)dx = \int_{\mathbb{R}} \frac{1}{\xi} \phi\left(\frac{t-s}{\xi}\right) dB(s), \quad \xi = \sqrt{\gamma^2 + \nu^2}. \quad (31)$$

Lemma 3. For the smoothed stationary Gaussian process $z_\gamma(t)$ defined in (31), the variances of its derivatives are given by

$$\begin{aligned}\text{Var}(z'_\gamma(t)) &= \frac{1}{4\sqrt{\pi}\xi^3}, & \text{Var}(z''_\gamma(t)) &= \frac{3}{8\sqrt{\pi}\xi^5}, \\ \text{Var}(z_\gamma^{(3)}(t)) &= \frac{15}{16\sqrt{\pi}\xi^7}, & \text{Var}(z_\gamma^{(4)}(t)) &= \frac{105}{32\sqrt{\pi}\xi^9}.\end{aligned}$$

Combining Lemma 3 and (29), we obtain immediately the following peak height distributions for the first and second derivatives of the smoothed process.

Proposition 2. Let $z_\gamma(t)$ be defined in (31). Then the peak height distributions of $z'_\gamma(t)$ and $z''_\gamma(t)$ are given respectively by

$$\begin{aligned}F_{z'_\gamma}(x) &= 1 - \Phi\left(\frac{x}{\sigma_1\sqrt{1-\eta_1^2}}\right) + \sqrt{2\pi}\eta_1\phi\left(\frac{x}{\sigma_1}\right)\Phi\left(\frac{\eta_1x}{\sigma_1\sqrt{1-\eta_1^2}}\right), \\ F_{z''_\gamma}(x) &= 1 - \Phi\left(\frac{x}{\sigma_2\sqrt{1-\eta_2^2}}\right) + \sqrt{2\pi}\eta_2\phi\left(\frac{x}{\sigma_2}\right)\Phi\left(\frac{\eta_2x}{\sigma_2\sqrt{1-\eta_2^2}}\right),\end{aligned}\tag{32}$$

where $\sigma_1^2 = \frac{1}{4\sqrt{\pi}\xi^3}$, $\eta_1 = \frac{\sqrt{3}}{\sqrt{5}}$, $\sigma_2^2 = \frac{3}{8\sqrt{\pi}\xi^5}$ and $\eta_2 = \frac{\sqrt{5}}{\sqrt{7}}$.

3.5 SNR and optimal bandwidth γ

Intuitively, a higher Signal-to-Noise Ratio (SNR) facilitates the detection of change points as it enhances the contrast between the signal and the noise. On the other hand, SNR is not only associated with the size of slope change and jump, but also a function of bandwidth γ . Thus, it is important to study the SNR when choosing the best bandwidth. The following result, which is a direct consequence of Lemmas 1 and 3, provides definitions and properties for SNR of both two types of change points.

Lemma 4. Assume that $z(t)$ is Gaussian white noise ($\nu = 0$ in (31)). For a Type I change point v_j , the SNR is calculated as

$$\text{SNR}_I(v_j) := \frac{|\mu''_\gamma(v_j)|}{\sqrt{\text{Var}(z''_\gamma(v_j))}} = \frac{\frac{|k_{j+1}-k_j|}{\sqrt{2\pi}\gamma}}{\sqrt{\frac{3}{8\sqrt{\pi}\gamma^5}}} = \frac{2\gamma^{3/2}}{\sqrt{3}\pi^{1/4}}|k_{j+1}-k_j|.\tag{33}$$

For a Type II change point v_j , it becomes asymptotically a local extremum at v_j under the condition (C2), and the corresponding SNR is calculated as

$$\begin{aligned} \text{SNR}_{\text{II}}(v_j) &:= \frac{|\mu'_\gamma(v_j) - k_j|}{\sqrt{\text{Var}(z'_\gamma(v_j))}} = \frac{|\frac{a_j}{\sqrt{2\pi}\gamma} + \frac{k_{j+1}-k_j}{2} + (k_j + k_{j+1})(\Phi(c) - 1)|}{\sqrt{\frac{1}{4\sqrt{\pi}\gamma^3}}} \\ &= \left| \frac{\sqrt{2}a_j}{\pi^{1/4}} \sqrt{\gamma} + [(k_{j+1} - k_j) + 2(k_j + k_{j+1})(\Phi(c) - 1)]\pi^{1/4}\gamma^{3/2} \right|. \end{aligned} \quad (34)$$

Due to the condition (C2) and $\Phi(c) \approx 1$, it is seen from (33) and (34) that two SNR's are increasing in sizes of slope change and jump, respectively. In addition, Lemma 4 shows the SNR is increasing in γ for both Type I and Type II change points. Therefore, if the minimal distance of neighbouring change points d is large enough, a large γ is preferable (see figure 5). However, for a fixed d , to avoid the overlap of two neighbouring smoothed signal segments $(v_j - c\gamma, v_j + c\gamma)$ and $(v_{j+1} - c\gamma, v_{j+1} + c\gamma)$, γ should not be too large (such as $2c\gamma \leq d$). Note that, it is assumed $\nu = 0$ in Lemma 4 to simplify the calculation; for the general case $\nu \neq 0$, similar results on γ can be obtained.

4 Simulation Study

4.1 Simulation settings

In this section, we will assess the performance of our method across various signal scenarios. The signals follow the form $\mu(t) = c_j + k_j t$, where $t = 1, \dots, L$. True change points are defined as $v_j = jd$ for $j = 1, \dots, \lfloor L/d \rfloor - 1$ with $d = 150$ representing the separation between adjacent change points. We consider four distinct signal scenarios: (1) piecewise linear mean with continuous change points (Type I change points); (2) piecewise constant mean with jumps (special case of Type II change points); (3) piecewise linear mean with discontinuous change points (Type II change points); (4) mixture of Type I and Type II change points. For the first three scenarios, let $L = 15,000$ and thus $J = 99$ for each scenario. For the mixture case, we extend the signal length to $L = 30,000$ with $J_1 = J_2 = 99$.

The noise is generated from a zero-mean stationary ergodic Gaussian process. It assumes a white noise when $\nu = 0$ and becomes correlated when $\nu > 0$. To generate the kernel smoothing data, we use the Gaussian kernel $w_\gamma(t) = (1/\gamma)\phi(t/\gamma)\mathbb{1}(t \in [-6\gamma, 6\gamma])$. To control the False Discovery Rate (FDR), we implement the Benjamini-Hochberg (BH) procedure at a significant level of $\alpha = 0.05$. Our simulation results are based on the averaging of 1,000 replications.

4.2 Performance of our method

In Section 3, we presented the theoretical results of False Discovery Rate (FDR) and power of our method. In this section, we validate these theoretical properties through numerical studies.

Figure 5 shows the performance of our method across the four different signal scenarios. Notably, as the Signal-to-Noise Ratio (SNR) increases, the FDR converges to its asymptotic limit. This limit consistently remains below the FDR control level of $\alpha = 0.05$. Meanwhile, the statistical power approaches 1. For a fixed bandwidth γ , a higher SNR implies a more substantial slope change or jump size, aligning with the conditions (C1) and (C2), respectively. It is worth noting that the conditions in our theoretical analysis assume an infinite SNR. However, our numerical results demonstrate that even when SNR is not exceptionally large (SNR is approximately 15 in our simulation), both the FDR and Power have already converged to their asymptotic limits.

4.2.1 Choice of bandwidth γ

Figure 6 illustrates the relationship between the kernel bandwidth γ , FDR and power. Notably, when γ is relative small, the performance of FDR and power improves as γ increases. This improvement is attributed to the fact that a larger γ results in a higher SNR, which, in turn, facilitates more accurate change point detection. A higher SNR corresponds to increased power in detecting true change points while effectively controlling the FDR. However, there is a trade-off. When γ becomes excessively large, it can lead to the issue of overlap. For example, the kernel region, defined by 12γ , may extend beyond the distance between neighboring change points v_j and v_{j+1} . This overlap

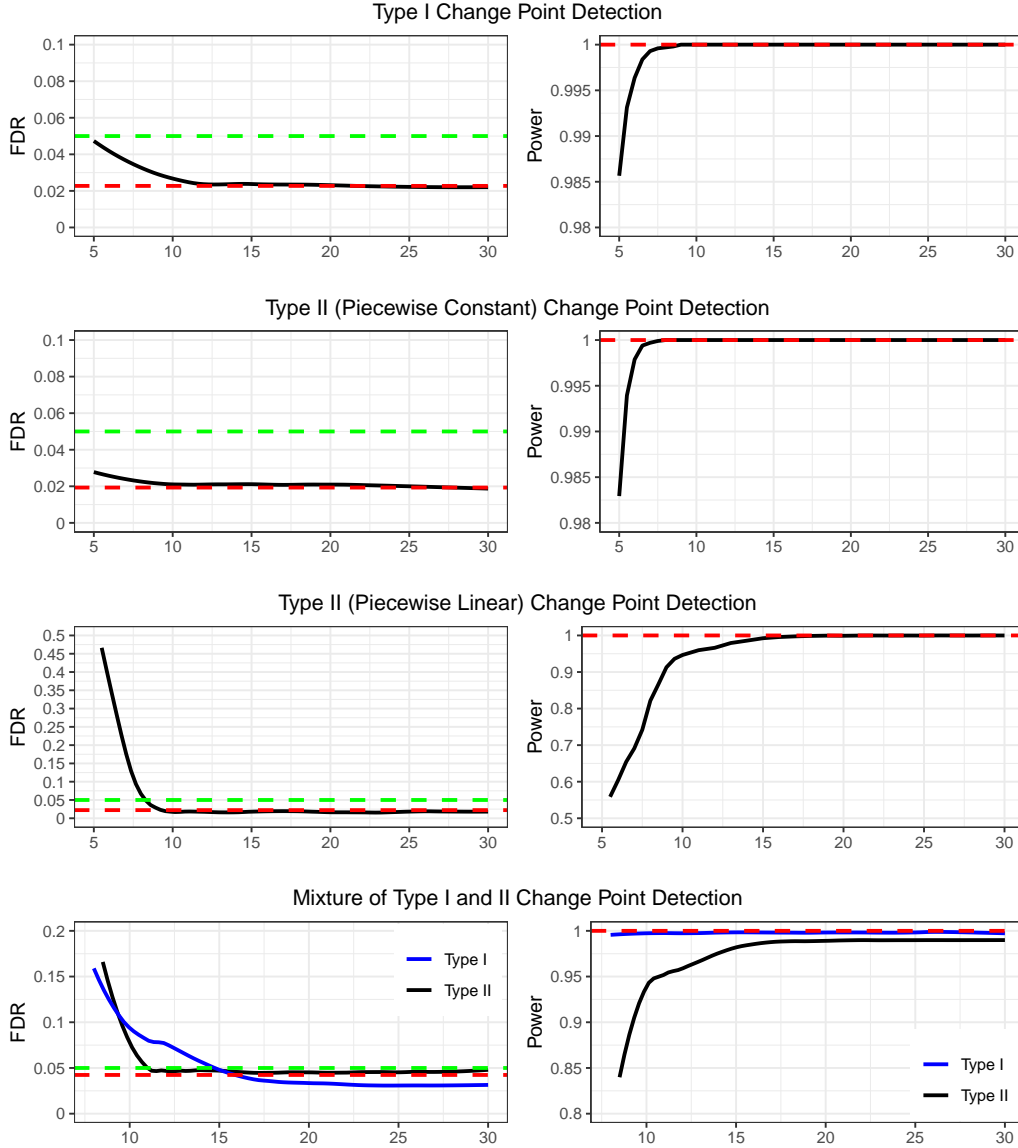


Figure 5: FDR (left panel) and power (right panel) versus Signal-to-Noise Ratio (SNR) for detecting change points in various signal types. This example employs a kernel bandwidth of $\gamma = 10$ and a location tolerance of $b = 10$. The red dashed lines mark the asymptotic limits of FDR and power, while the green dashed lines indicate the significant level $\alpha = 0.05$.

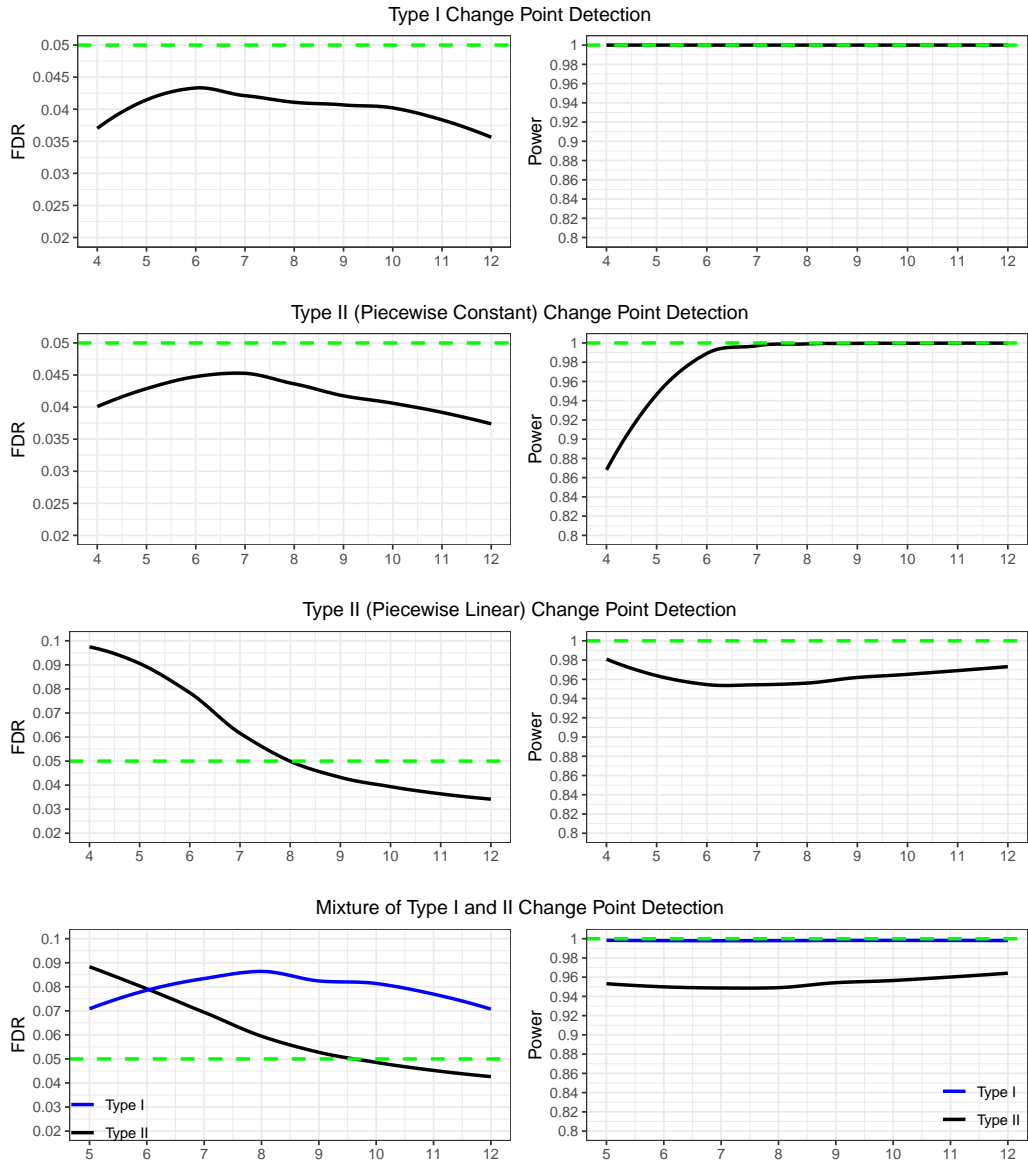


Figure 6: The FDR (left panel) and Power (right panel) versus the bandwidth γ for detecting change points in various signal types. In this example, the kernel bandwidth γ is varied between 4 and 12, with a fixed location tolerance of $b = 10$. The green dashed lines indicate the FDR control level, set at $\alpha = 0.05$ for FDR plots and at 1 for power plots.

can introduce distortions and complicate the detection of individual change points. Given these considerations, our simulation results suggest that $\gamma = 12$ is a recommended choice.

4.3 Comparison with other methods

To compare with other change point detection methods, we evaluated the precision and computational efficiency of change point detection. Both short-term (see the section 4.1) and long-term data sequences were considered. The extended long-term data sequence was generated by replicating the short-term data tenfold within our simulation, guaranteeing that the underlying patterns remained consistent between the two datasets.

We compared our method with some multiple testing-based change point detection methods: B&P (Bai, 1997), NOT (Baranowski et al., 2019), and NSP (Fryzlewicz, 2023). Note that we excluded the results of B&P method from the long-term data comparison due to the extremely long computing time. For the NSP method, change points were estimated as confidence intervals, and we used the midpoints of these intervals as point estimates for comparison with other methods for the sake of consistency. Additionally, the scenario of mixture of Type I and Type II change points was not considered, because the other three methods can not distinguish between Type I and Type II change points.

Suppose the number of true change points is J , and the number of detected change points is \hat{J} . For each detected change point \hat{v}_i , $i = 1, 2, \dots, \hat{J}$, we define it as the estimate of the true change point v_j such that

$$j = \operatorname{argmin}_{j=1,2,\dots,J} |\hat{v}_i - v_j|. \quad (35)$$

For simplicity, let $v_i^0 = v_j$ be the true change point corresponding to \hat{v}_i , where j is defined in (35). Note that a single true change point can correspond to multiple estimated change points. The detection accuracy of \hat{v}_i is measured based on the distance $|\hat{v}_i - v_i^0|$ for $i = 1, 2, \dots, \hat{J}$, which is represented as the capture rate in Tables 1 and 2.

In Table 1, the results for short-term data illustrate the performance of our proposed method, NOT and NSP in terms of FDR control and power across all scenarios. Both NOT and our method demonstrate the capability to achieve high accuracy in change point detection within a single bandwidth γ , and our method is the fastest among the algorithms considered. In Table 2, it is seen that for the long-term data sequence, NOT and NSP do not perform well regarding the FDR control, power and detection accuracy. In contrast, our method consistently maintains excellent performance, retaining the advantage of the shortest computing time.

It is worth noting that our method’s slightly better performance in terms of FDR and power with long-term data can be attributed to the asymptotic conditions $L \rightarrow \infty$ and $J/L \rightarrow A > 0$. Additionally, the minimal computing time required by our method in both short-term and long-term data sequences demonstrates its superior computation complexity.

5 Data examples

In this section, we applied our method to real applications and conducted a comparative analysis with NOT and NSP (B&P method was excluded due to its poor performance and extensive computing time). We evaluated the performance of all three methods on two distinct datasets: one featuring global temperature records (short-term), and the other involving the stock price of a hotel company (long-term).

5.1 Global temperature records

Climate change research plays a pivotal role in addressing the impacts of global warming and guiding policy decisions related to mitigation and adaptation strategies. Analyzing temperature change is crucial for understanding the patterns and shifts in climate over time.

In this paper, we studied the data concerning global mean land-ocean temperature deviations (measured in degrees centigrade) from the period 1880 to 2015, in comparison to the average tem-

Table 1: Detection accuracy of change points for the short-term data sequence ($\gamma = 10$ and $b = \gamma$). The capture rate of an interval I is defined as $\sum_{i=1}^J \mathbb{1}(|\hat{v}_i - v_i^0| \in I)/J$, where v_i^0 is the true change point corresponding to the detected change point \hat{v}_i .

Signal Type	Method	Capture rate of interval					FDR	Power	Time (s)
		$[0, \frac{1}{3}\gamma)$	$[\frac{1}{3}\gamma, \gamma)$	$[\gamma, 2\gamma)$	$[2\gamma, 4\gamma)$	$\geq 4\gamma$			
Type I	mSTEM	0.8400	0.1533	0.0217	0.0267	0.0483	0.0125	0.9933	0.1370
	NOT	0.9883	0.0117	0.0000	0.0017	0.0000	0.0572	1.0000	1.3550
	NSP	0.6183	0.1900	0.1617	0.0300	0.0000	0.0458	0.9999	3.2417
	B&P	0.4700	0.5083	0.0217	0.0000	0.0000	0.1632	0.9783	87.4562
Type II	mSTEM	0.9617	0.0383	0.0000	0.0367	0.0333	0.0227	1.0000	0.0290
	NOT	0.9833	0.0183	0.0017	0.0000	0.0017	0.0558	1.0000	0.2863
Piecewise Constant	NSP	0.6767	0.3133	0.2117	0.0867	0.0100	0.0517	0.9001	1.9430
	B&P	0.4117	0.0233	0.0467	0.2050	0.0000	0.1260	0.4350	71.0924
Type II	mSTEM	0.9983	0.0017	0.0000	0.0067	0.0233	0.0348	1.0000	0.0839
	NOT	0.8833	0.0933	0.0233	0.0000	0.0000	0.0727	0.9766	0.4524
Piecewise Linear	NSP	0.6967	0.2417	0.0333	0.0283	0.0000	0.0626	0.9384	2.8013
	B&P	0.3333	0.0000	0.3015	0.3333	0.0745	0.1633	0.3333	68.3345

perature between 1951 and 1980. This dataset is available at <https://data.giss.nasa.gov/gistemp/graphs>.

Figure 7 illustrates the results of applying all three methods to the global temperature data. Our method successfully detected two Type II change points in 1902 and 1934, along with one Type I change point in 1971. These findings closely align with the results presented in a prior study by Yu and Ruggieri (2019), where they conducted an analysis of five time series and identified three distinct periods of significant temperature change in the 20th century. Specifically, their research highlighted change points between 1902-1917, 1936-1945 and 1963-1976. Indeed, the result of

Table 2: Detection accuracy of change points for the long-term data sequence ($\gamma = 10$ and $b = \gamma$). The proportion of an interval I is defined as $\sum_{i=1}^J \mathbb{1}(|\hat{v}_i - v_i^0| \in I)/J$, where v_i^0 is the true change point corresponding to the detected change point \hat{v}_i .

Signal Type	Method [†]	Capture rate of interval					FDR	Power	Time (s)
		$[0, \frac{1}{3}\gamma)$	$[\frac{1}{3}\gamma, \gamma)$	$[\gamma, 2\gamma)$	$[2\gamma, 4\gamma)$	$\geq 4\gamma$			
Type I	mSTEM	0.7616	0.2241	0.0295	0.0244	0.0135	0.0127	0.9963	0.2469
	NOT	0.1358	0.1712	0.2475	0.5028	0.2369	0.0853	0.8732	112.5007
	NSP	0.3512	0.4607	0.1692	0.0086	0.0000	0.0792	0.8362	433.6193
Type II Piecewise Constant	mSTEM	0.9702	0.0000	0.000	0.0154	0.0161	0.01463	1.0000	0.1188
	NOT	0.8633	0.0037	0.007	0.0177	0.0090	0.0735	0.9164	48.4487
	NSP	0.6398	0.3202	0.030	0.0000	0.0000	0.08011	0.9228	213.0398
Type II Piecewise Linear	mSTEM	0.9899	0.0000	0.0000	0.0065	0.0133	0.0237	0.9992	1.0627
	NOT	0.8748	0.0002	0.0009	0.0032	0.0025	0.1217	0.8012	10.6064
	NSP	0.6059	0.3543	0.0298	0.0000	0.0000	0.1383	0.8255	400.6633

[†] B&P method was not included due to its substantial computational time requirements.

our detection method aligns with the visual assessment of the data sequence. The observed pattern suggests that the signal remained relatively constant during the first period (1880 - 1902), followed by a linear trend in the second period (1903 - 1934), then another constant signal in the third period (1935 - 1971), and finally a linear trend in the last period.

5.2 Stock price of Host Hotel & Resorts, Inc.

Through analyzing the daily stock price of Host Hotel & Resorts, Inc. (HST) from January 1, 2018, to November 5, 2021, one can provide valuable insights into the company's stock performance and uncover any significant change points that may have occurred during this period. As the world's largest lodging and real estate investment trust (REIT), HST's stock price can be influ-

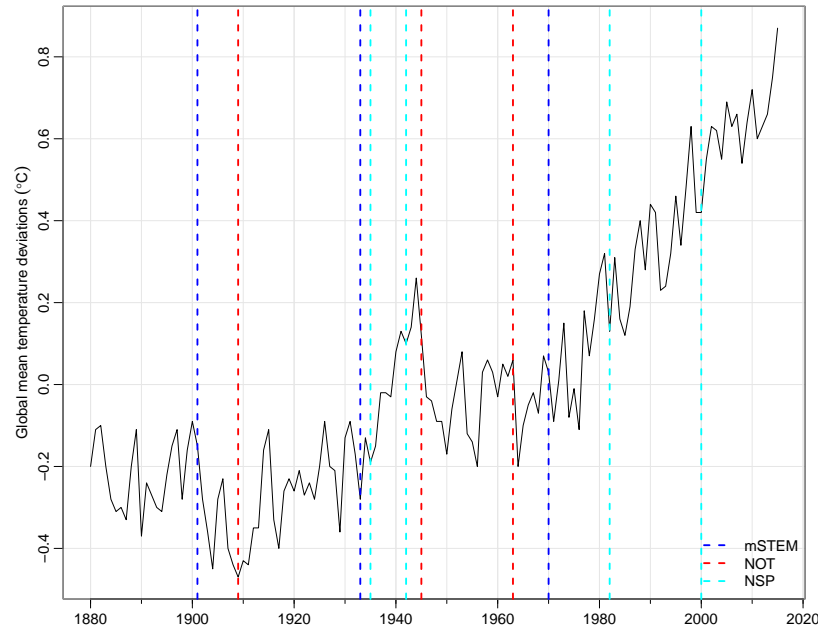


Figure 7: Change point detection of global mean land-ocean temperature deviations from 1880 to 2015. Our method detects three change points: 1902 (Type II), 1934 (Type II) and 1971 (Type I). NOT detects three change points: 1910, 1946 and 1964; NSP identifies four change points: 1936, 1943, 1983 and 2001.

enced by various factors, including market conditions, industry trends, company-specific events and macroeconomic factors. The historical data for HST stock price is available at <https://finance.yahoo.com>.

The application of our method to detect the change points in the HST stock price allows for the identification of periods characterized by significant shifts in the stock's behavior or trends. These change points may correspond to specific events or factors that affect HST's stock price, such as earnings releases, mergers and acquisitions, changes in industry regulations and market-moving news.

Figure 8 shows the results of change point detection for the HST stock price. It is seen that NOT and NSP, particularly NSP, tend to be sensitive to variations in the time series, resulting in the detection of numerous local extrema that can be attributed to noise. This leads to a higher False

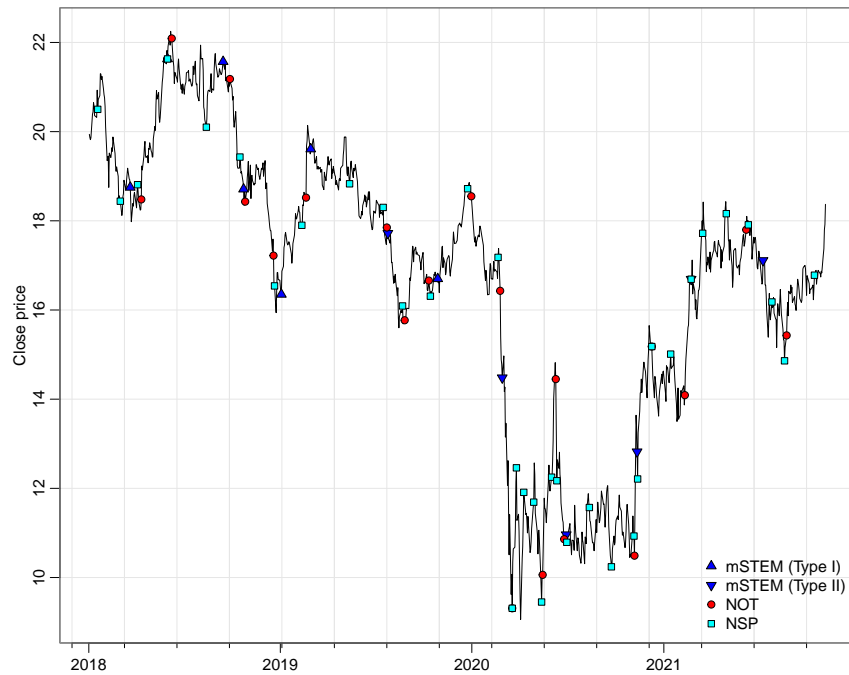


Figure 8: Change point detection of HST stock price (January 1, 2018 - November 5, 2020).

Discover Rate (FDR). In contrast, our method provides detection results that are more interpretable. The detected change points align with big events, such as the outbreak of trade war between the USA and China in 2018 - 2019, which had a notable impact on the S&P 500 and other large-cap stocks. Similarly, the detected change points after 2020 correspond to the timeline of the Covid-19 outbreak, which significantly affected the global tourist industry.

6 Discussion

6.1 Choice of smoothing bandwidth γ

The choice of the smoothing bandwidth γ is indeed an important aspect of change point detection. It plays a role in balancing the trade-off between overlapping of the smoothed signal supports and accuracy of detecting change points. Thus, either a small γ (if the noise is highly autocorrelated) or a relatively large γ (if the noise is less autocorrelated) is preferred in order to increase power, but

only to the extent that the smoothed signal supports have little overlap. Considering the Gaussian kernel with support domain of $\pm c\gamma$, an initial guideline for choosing γ can be set it as $b = d/(2c)$, where d is the minimal distance between any two neighboring change points. This guideline ensures that the supports of the smoothed signals do not overlap excessively. For example, if we consider the Gaussian kernel to have an effective support of $\pm 4\gamma$ and $d = 100$, we may choose γ to be no larger than $\gamma = 12$.

It is worth noting that the choice of γ may require an iterative procedure, especially when the distance between change points is unknown. A more precise optimization needs to be performed by iteratively adjusting the value of γ and evaluating the detection performance. Moreover, in some cases where the change points are not uniformly distributed and some are close together while others are far apart, an adaptive bandwidth that varies across the signal may be preferable to effectively capture both closely spaced and widely spaced change points. We leave these as problems for future research.

6.2 Type II change points with moderate $|q_j|$

For a Type II change point v_j , we have studied in this paper the case of small $|q_j|$, and showed in Remark 2 the case of large $|q_j|$ that it behaves similarly to a Type I change point. But when a Type II change point has moderate $|q_j|$, for example $|q_j|$ is close to c/γ , the first derivative $\mu'_\gamma(t)$ can produce a local extremum at $t = v_j \pm \gamma^2|q_j| \approx v_j \pm c\gamma$, which is near the endpoints of the smoothed signal region and outside of $v_j \pm b$. This may cause a false detection in the noise region while missing detecting v_j in the signal region, leading to overestimation of FDR and underestimation of power.

Addressing this limitation of detecting Type II change points with moderate $|q_j|$ would be an interesting question for future research. It may involve developing additional theoretical insights and modifying our proposed method mSTEM to enhance its ability to handle a wider range change points scenarios.

6.3 Extension to multivariate linear models

A univariate linear model is assumed to formulate the signal-plus-noise in this paper, but our proposed method can be extended to the multivariate linear models (Bai and Safikhani, 2022; Chen and Gupta, 2012). For example, we are interested in the following p -dimensional linear model and detecting possible change points:

$$y_t = \mu_t + z_t = X_t \boldsymbol{\beta}^{(j)} + z_t, \text{ for } t \in (v_{j-1}, v_j], j = 1, 2, \dots \quad (36)$$

where $X_t = (1, X_{1t}, \dots, X_{pt})^T$ is the covariate vector and $\boldsymbol{\beta}^{(j)} = (\beta_0^{(j)}, \beta_1^{(j)}, \dots, \beta_p^{(j)})^T \in \mathbb{R}^{p+1}$. When $p = 1$, by letting $\boldsymbol{\beta}^{(j)} = (\beta_0^{(j)}, \beta_1^{(j)})^T = (c_j, k_j)^T$ for $t \in (v_{j-1}, v_j]$, $j = 1, 2, \dots$, and $X_{1t} = t$, (36) becomes the univariate piecewise linear model $y_t = c_j + k_j t + z_t$.

To estimate the number and location of change points simultaneously, our mSTEM method can still be applied to each dimension independently. Specifically, suppose we have T realizations $\{(y_t, X_t), t = 1, \dots, T\}$, for each dimension $m = 1, \dots, p$, the first and second derivatives of $\mu_{\gamma t}$ are studied, and suppose the detected change points are $\boldsymbol{v}^{(m)} = (v_1^{(m)}, \dots, v_{n_m}^{(m)})$, where n_m is the number of detected change points for the m -th dimension. It is possible that some change points occur at similar or exactly the same locations across different dimensions. For example, in dimension i and j , $i \neq j$, some locations in $\boldsymbol{v}^{(i)}$ and $\boldsymbol{v}^{(j)}$ will be very close, we consider these change points to be the result of the same underlying change points.

6.4 Nonstationary Gaussian noise

In this paper, the Gaussian noise is assumed to be stationary, which allows the error terms can be correlated. However, in real applications, it is common that the data contains nonstationary Gaussian noise (Heinonen et al., 2016; Phoon et al., 2005). Thus, it is interesting and valuable to investigate change point detection under nonstationary Gaussian noise. To achieve this, we will study the peak height distribution for nonstationary Gaussian noise and show the FDR control and power consistency under certain assumptions, which would be promising but with certain challenges.

Supplementary Materials

The supplementary materials contain proofs of all technical results in the paper.

Acknowledgements

The authors thank professor Armin Schwartzman (University of California San Diego) for helpful discussions and suggestions.

Funding

D.C. acknowledges support from National Science Foundation grant DMS-2220523 and Simons Foundation Collaboration Grant 854127.

Supplementary Materials

Proof of Lemma 2. Note that, if $a_j = 0$, then $\mu'_\gamma(t)$ is monotone in $(v_j - c\gamma, v_j + c\gamma)$ and hence there is no local extremum. If $a_j \neq 0$, by letting $\mu''_\gamma(t) = 0$, we see that the local extremum of $\mu'_\gamma(t)$ is achieved at $t = v_j + \gamma^2 q_j$. Similarly, solving the equation

$$\mu_\gamma^{(3)}(t) = \left[\frac{a_j}{\gamma^3} + \frac{a_j(v_j - t) + (k_{j+1} - k_j)\gamma^2}{\gamma^3} \frac{v_j - t}{\gamma^2} \right] \phi\left(\frac{v_j - t}{\gamma}\right) = 0,$$

we obtain that the local extremum of $\mu'_\gamma(t)$ is achieved at

$$t = \begin{cases} v_j + \frac{\gamma^2 q_j \pm \gamma \sqrt{4 + q_j^2 \gamma^2}}{2} & a_j \neq 0, \\ v_j & a_j = 0. \end{cases}$$

□

A Peak Height Distributions for $z'_\gamma(t)$ and $z''_\gamma(t)$

Proof of Lemma 3 and Proposition 2. Due to the stationarity of $z_\gamma(t)$, without loss of generality, we only consider the case when $t = 0$. The variances of $z_\gamma^{(d)}(0)$, $d = 1, \dots, 4$, are calculated as follows.

$$\begin{aligned} \text{Var}(z'_\gamma(0)) &= \int_{\mathbb{R}} \frac{s^2}{\xi^6} \phi^2\left(\frac{s}{\xi}\right) ds = \frac{1}{\xi^6} \frac{\xi}{2\sqrt{\pi}} \int_{\mathbb{R}} s^2 \frac{\sqrt{2}}{\xi} \phi\left(\frac{s}{\xi/\sqrt{2}}\right) ds \\ &= \frac{1}{\xi^6} \frac{\xi}{2\sqrt{\pi}} \frac{\xi^2}{2} = \frac{1}{4\sqrt{\pi}\xi^3}; \end{aligned}$$

$$\begin{aligned} \text{Var}(z''_\gamma(0)) &= \int_{\mathbb{R}} \frac{1}{\xi^6} \phi^2\left(\frac{s}{\xi}\right) ds - 2 \int_{\mathbb{R}} \frac{s^2}{\xi^8} \phi^2\left(\frac{s}{\xi}\right) ds + \int_{\mathbb{R}} \frac{s^4}{\xi^{10}} \phi^2\left(\frac{s}{\xi}\right) ds \\ &= \frac{1}{\xi^4} \frac{1}{2\sqrt{\pi}\xi} - \frac{2}{\xi^2} \frac{1}{4\sqrt{\pi}\xi^3} + \frac{1}{\xi^{10}} \frac{\xi}{2\sqrt{\pi}} \int_{\mathbb{R}} s^4 \frac{\xi}{\sqrt{2}} \phi\left(\frac{s}{\xi/\sqrt{2}}\right) ds \\ &= \frac{1}{\xi^{10}} \frac{\xi}{2\sqrt{\pi}} \frac{3\xi^4}{4} = \frac{3}{8\sqrt{\pi}\xi^5}; \end{aligned}$$

$$\begin{aligned}
\text{Var}(z_\gamma^{(3)}(0)) &= 9 \int_{\mathbb{R}} \frac{s^2}{\xi^{10}} \phi^2\left(\frac{s}{\xi}\right) ds - 6 \int_{\mathbb{R}} \frac{s^4}{\xi^{12}} \phi^2\left(\frac{s}{\xi}\right) ds + \int_{\mathbb{R}} \frac{s^6}{\xi^{14}} \phi^2\left(\frac{s}{\xi}\right) ds \\
&= \frac{9}{\xi^4} \frac{1}{4\sqrt{\pi}\xi^3} - \frac{6}{\xi^2} \frac{3}{8\sqrt{\pi}\xi^5} + \frac{1}{\xi^{14}} \frac{\xi}{2\sqrt{\pi}} \int_{\mathbb{R}} s^6 \frac{\sqrt{2}}{\xi} \phi\left(\frac{s}{\xi/\sqrt{2}}\right) ds \\
&= \frac{1}{\xi^{14}} \frac{\xi}{2\sqrt{\pi}} \frac{15\xi^6}{8} = \frac{15}{16\sqrt{\pi}\xi^7};
\end{aligned}$$

$$\begin{aligned}
\text{Var}(z_\gamma^{(4)}(0)) &= 9 \int_{\mathbb{R}} \frac{1}{\xi^{10}} \phi^2\left(\frac{s}{\xi}\right) ds - 36 \int_{\mathbb{R}} \frac{s^2}{\xi^{12}} \phi^2\left(\frac{s}{\xi}\right) ds + 42 \int_{\mathbb{R}} \frac{s^4}{\xi^{14}} \phi^2\left(\frac{s}{\xi}\right) ds \\
&\quad - 12 \int_{\mathbb{R}} \frac{s^6}{\xi^{16}} \phi^2\left(\frac{s}{\xi}\right) ds + \int_{\mathbb{R}} \frac{s^8}{\xi^{18}} \phi^2\left(\frac{s}{\xi}\right) ds \\
&= \frac{1}{\xi^9} \left(9 \times \frac{1}{2\sqrt{\pi}} - 36 \times \frac{1}{4\sqrt{\pi}} + 42 \times \frac{3}{8\sqrt{\pi}} - 12 \times \frac{15}{16\sqrt{\pi}} + \frac{1}{2\sqrt{\pi}} \times \frac{105}{16} \right) \\
&= \frac{105}{32\sqrt{\pi}\xi^9}.
\end{aligned}$$

Hence, the parameters of the peak height distributions for $z'_\gamma(t)$ and $z''_\gamma(t)$ are given respectively by

$$\begin{aligned}
\sigma_1^2 = \text{Var}(z'_\gamma(0)) &= \frac{1}{4\sqrt{\pi}\xi^3}, & \eta_1 &= \frac{\text{Var}(z''_\gamma(0))}{\sqrt{\text{Var}(z'_\gamma(0))\text{Var}(z_\gamma^{(3)}(0))}} = \frac{\sqrt{3}}{\sqrt{5}}; \\
\sigma_2^2 = \text{Var}(z''_\gamma(0)) &= \frac{3}{8\sqrt{\pi}\xi^5}, & \eta_2 &= \frac{\text{Var}(z_\gamma^{(3)}(0))}{\sqrt{\text{Var}(z''_\gamma(0))\text{Var}(z_\gamma^{(4)}(0))}} = \frac{\sqrt{5}}{\sqrt{7}}.
\end{aligned}$$

This leads to the desired peak height distributions in Proposition 2. \square

B FDR Control and Power Consistency for Type I Change Points

Proof of Theorem 1. Note that Type I change points are detected using the second derivative $y''_\gamma(t) = \mu''_\gamma(t) + z''_\gamma(t)$, where a change point v_j becomes a local extremum in $\mu''_\gamma(t)$ precisely at v_j by Proposition 1 and $z''_\gamma(t)$ is a smooth Gaussian process. Moreover, $\mu'(t)$ is piecewise constant with size of jump $|k_{j+1} - k_j|$ at v_j . Thus the detection of Type I change points using the second derivative is essentially equivalent to the detection of change points in piecewise constant signals (Cheng et al., 2020). Under condition (C1), by substituting the original signal μ with μ' and replacing the differential smoothed noise z'_γ with z''_γ , we see that Theorem 1 follows from Theorems 3.1 and 3.3 in Cheng et al. (2020). \square

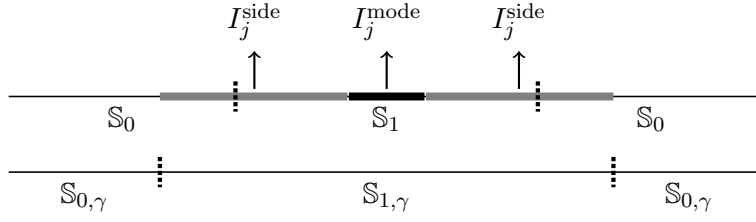


Figure 9: Illustration of the *signal region* \mathbb{S}_1 (S_j in this example), *null region* \mathbb{S}_0 , *smoothed signal region* $\mathbb{S}_{1,\gamma}$ ($S_{j,\gamma}$ in this example) and *smoothed null region* $\mathbb{S}_{0,\gamma}$.

I_j^{mode} and I_j^{side} are a partition of $S_{j,\gamma}$ such that $I_j^{\text{mode}} \subset S_j \subset S_{j,\gamma}$.

C Supporting Results for FDR Control and Power Consistency for Type II Change Points

To prove Theorem 2 and Theorem 3, we require the following lemmas in this section. It is important to note that the lemmas provided below are based on Type II change points detection, where $a_j \neq 0$.

Recall that the *signal region* is defined as $\mathbb{S}_1 = \cup_{j=1}^J S_j = \cup_{j=1}^J (v_j - b, v_j + b)$, and the smoothed signal is generated by convolving the signal and a kernel function with support $[-c\gamma, c\gamma]$. Hence, the *smoothed signal region* is $\mathbb{S}_{1,\gamma} = \cup_{j=1}^J S_{j,\gamma} = \cup_{j=1}^J (v_j - c\gamma, v_j + c\gamma)$, where $S_{j,\gamma}$ is the smoothed signal region of change point v_j (see Figure 9).

Lemma S1. *Let $I_j^{\text{side}} \cup I_j^{\text{mode}} = (v_j - c\gamma, v_j + c\gamma) = S_{j,\gamma}$ be a partition of $S_{j,\gamma}$, where $I_j^{\text{mode}} := \{t \in U(L) : |t - v_j| \leq \delta\}$ and $0 < \delta < \min\{b, \gamma\}$ such that $I_j^{\text{mode}} \subset S_j$. If $q = \sup_j |q_j|$ is sufficiently small, then*

(1). $M_\gamma = \inf_j M_{j,\gamma} > 0$, where $M_{j,\gamma} = \inf_{I_j^{\text{mode}}} \frac{|\mu'_\gamma(t) - k(t)|}{|a_j|}$ and $k(t)$ is the slope at t .

(2). $C_\gamma = \inf_j C_{j,\gamma} > 0$, where $C_{j,\gamma} = \frac{1}{|a_j|} \inf_{I_j^{\text{side}}} |\mu''_\gamma(t)|$.

(3). $D_\gamma = \inf_j D_{j,\gamma} > 0$, where $D_{j,\gamma} = \frac{1}{|a_j|} \inf_{I_j^{\text{mode}}} |\mu_\gamma^{(3)}(t)|$.

Proof. (1). It follows from the arguments of Lemma 1 that

$$\begin{aligned}\frac{\mu'_\gamma(t) - k(t)}{a_j} &= \frac{1}{a_j} \left[\frac{a_j}{\gamma} \phi\left(\frac{v_j - t}{\gamma}\right) - (k_{j+1} - k_j) \Phi\left(\frac{v_j - t}{\gamma}\right) + k_{j+1} \right] - \frac{k(t)}{a_j} \\ &= \frac{1}{\gamma} \phi\left(\frac{v_j - t}{\gamma}\right) - q_j \Phi\left(\frac{v_j - t}{\gamma}\right) + \frac{k_{j+1} - k(t)}{a_j}.\end{aligned}$$

For $t \in I_j^{\text{mode}}$, $(k_{j+1} - k(t))/a_j = 0$ or q_j as $k(t) = k_j$ or k_{j+1} . If q is sufficiently small, then $M_{j,\gamma} > 0$ and it follows that $M_\gamma = \inf_j M_{j,\gamma} > 0$.

(2). Note that $t \in I_j^{\text{side}} \subset S_{j,\gamma}$ implies $\delta < |v_j - t| < c\gamma$. By Lemma 1,

$$C_{j,\gamma} = \frac{1}{|a_j|} \inf_{I_j^{\text{side}}} |\mu''_\gamma(t)| = \inf_{I_j^{\text{side}}} \left| \frac{(v_j - t) + q_j \gamma^2}{\gamma^3} \phi\left(\frac{v_j - t}{\gamma}\right) \right|.$$

If q is sufficiently small, then $C_{j,\gamma} > 0$ and $C_\gamma = \inf_j C_{j,\gamma} > 0$.

(3). For $t \in I_j^{\text{mode}}$, it follows from the proof of Lemma 2 that

$$D_{j,\gamma} = \frac{1}{|a_j|} \inf_{I_j^{\text{mode}}} |\mu_\gamma^{(3)}(t)| = \inf_{I_j^{\text{mode}}} \left| \frac{1}{\gamma^3} + \frac{(v_j - t)^2 + q_j(v_j - t)\gamma^2}{\gamma^5} \phi\left(\frac{v_j - t}{\gamma}\right) \right|.$$

If q is sufficiently small, then $D_{j,\gamma} > 0$ and $D_\gamma = \inf_j D_{j,\gamma} > 0$. □

To simplify the notations below, we regard $\tilde{T}_\Pi \cap I_j^{\text{side}}$ as $\tilde{T}_\Pi^+ \cap I_j^{\text{side}}$ if $j \in \mathcal{I}_\Pi^+$ and as $\tilde{T}_\Pi^- \cap I_j^{\text{side}}$ if $j \in \mathcal{I}_\Pi^-$, respectively. The same notation applies accordingly when \tilde{T}_Π is replaced with $\tilde{T}_\Pi(u)$ or when I_j^{side} is replaced with I_j^{mode} .

Lemma S2. *For a Type II change point v_j , suppose that $q = \sup_j |q_j|$ is sufficiently small, then $\mu'_\gamma(t)$ has a local extremum at $t = v_j + \gamma^2 q_j \in I_j^{\text{mode}}$. Let $\sigma_1 = sd(z'_\gamma(t))$, $\sigma_2 = sd(z''_\gamma(t))$ and $\sigma_3 = sd(z_\gamma^{(3)}(t))$. Then*

$$(1). P(\#\{t \in \tilde{T}_\Pi \cap I_j^{\text{side}}\} = 0) \geq 1 - \exp\left(-\frac{a_j^2 C_{j,\gamma}^2}{2\sigma_2^2}\right).$$

$$(2). P(\#\{t \in \tilde{T}_\Pi \cap I_j^{\text{mode}}\} = 1) \geq -1 + 2\Phi\left(\frac{|a_j| C_{j,\gamma}}{\sigma_2}\right) - \exp\left(-\frac{a_j^2 D_{j,\gamma}^2}{2\sigma_3^2}\right).$$

$$(3). P(\#\{t \in \tilde{T}_\Pi(u) \cap I_j^{\text{mode}}\} = 1) \geq 1 - \exp\left(-\frac{a_j^2 D_{j,\gamma}^2}{2\sigma_3^2}\right) - \Phi\left(\frac{u - |a_j| M_{j,\gamma}}{\sigma_1}\right) \text{ for any fixed } u.$$

Proof. (1). As the probability that there are no local extremum of $y'_\gamma(t)$ in I_j^{side} is greater than the probability that $|y''_\gamma(t)| > 0$ for all $t \in I_j^{\text{side}}$, we have

$$\begin{aligned}
P(\#\{t \in \tilde{T}_{\text{II}} \cap I_j^{\text{side}}\} = 0) &\geq P(\inf_{I_j^{\text{side}}} |y''_\gamma(t)| > 0) \\
&\geq P(\sup_{I_j^{\text{side}}} |z''_\gamma(t)| < \inf_{I_j^{\text{side}}} |\mu''_\gamma(t)|) \\
&= 1 - P(\sup_{I_j^{\text{side}}} |z''_\gamma(t)| > \inf_{I_j^{\text{side}}} |\mu''_\gamma(t)|) \\
&\geq 1 - \exp\left(-\frac{a_j^2 C_{j,\gamma}^2}{2\sigma_2^2}\right),
\end{aligned} \tag{C.37}$$

where the last line holds due to the Borell-TIS inequality.

(2). Consider here $j \in \mathcal{I}_{\text{II}}^+$ since the case of $j \in \mathcal{I}_{\text{II}}^-$ is similar. The probability that $y'_\gamma(t)$ has no local maximum in I_j^{mode} is less than the probability that $y''_\gamma(v_j - \delta) \leq 0$ or $y''_\gamma(v_j + \delta) \geq 0$. Thus the probability of no local maximum in I_j^{mode} is bounded above by

$$\begin{aligned}
P(\#\{t \in \tilde{T}_{\text{II}}^+ \cap I_j^{\text{mode}}\} = 0) &\leq P(y''_\gamma(v_j - \delta) \leq 0 \cup y''_\gamma(v_j + \delta) \geq 0) \\
&\leq P(y''_\gamma(v_j - \delta) \leq 0) + P(y''_\gamma(v_j + \delta) \geq 0) \\
&= \Phi\left(-\frac{\mu''_\gamma(v_j - \delta)}{\sigma_2}\right) + \Phi\left(\frac{\mu''_\gamma(v_j + \delta)}{\sigma_2}\right) \\
&= 1 - \Phi\left(\frac{\mu''_\gamma(v_j - \delta)}{\sigma_2}\right) + 1 - \Phi\left(-\frac{\mu''_\gamma(v_j + \delta)}{\sigma_2}\right) \\
&\leq 2 - 2\Phi\left(\frac{|a_j|C_{j,\gamma}}{\sigma_2}\right),
\end{aligned}$$

where the last line holds because $\mu''_\gamma(v_j - \delta) \geq |a_j|C_{j,\gamma} > 0$ and $-\mu''_\gamma(v_j + \delta) \geq |a_j|C_{j,\gamma} > 0$.

On the other hand, the probability that $y'_\gamma(t)$ has at least two local maxima in I_j^{mode} is less than the probability that $y_\gamma^{(3)}(t) > 0$ for some $t \in I_j^{\text{mode}}$ and $y_\gamma^{(3)}(t) < 0$ for some other $t \in I_j^{\text{mode}}$. Thus for $t \in \tilde{T}_{\text{II}}^+ \cap I_j^{\text{mode}}$,

$$\begin{aligned}
P(\#\{t \in \tilde{T}_{\text{II}}^+ \cap I_j^{\text{mode}}\} \geq 2) &\leq P(\sup y_\gamma^{(3)}(t) > 0 \cap \inf y_\gamma^{(3)}(t) < 0) \\
&\leq P(\sup y_\gamma^{(3)}(t) > 0) \wedge P(\inf y_\gamma^{(3)}(t) < 0) \\
&\leq P(\sup z_\gamma^{(3)}(t) > \inf -\mu_\gamma^{(3)}(t)) \wedge P(\sup z_\gamma^{(3)}(t) > \inf \mu_\gamma^{(3)}(t)) \\
&\leq \exp\left(-\frac{a_j^2 D_{j,\gamma}^2}{2\sigma_3^2}\right),
\end{aligned}$$

The last line holds due to Lemma S1.

The probability that $y'_\gamma(t)$ has only one local maximum in I_j^{mode} is calculated as

$$\begin{aligned}
& P(\#\{t \in \tilde{T}_{\text{II}}^+ \cap I_j^{\text{mode}}\} = 1) \\
&= 1 - P(\#\{t \in \tilde{T}_{\text{II}}^+ \cap I_j^{\text{mode}}\} = 0) - P(\#\{t \in \tilde{T}_{\text{II}}^+ \cap I_j^{\text{mode}}\} \geq 2) \quad (\text{C.38}) \\
&\geq -1 + 2\Phi\left(\frac{|a_j|C_{j,\gamma}}{\sigma_2}\right) - \exp\left(-\frac{a_j^2 D_{j,\gamma}^2}{2\sigma_3^2}\right).
\end{aligned}$$

(3). Consider first $j \in \mathcal{I}_{\text{II}}^+$. Since the probability that at least two local maxima of $y'_\gamma(t)$ in I_j^{mode} exceeding $u + k(t)$ is less than the probability that $y'_\gamma(t)$ has at least two maxima in I_j^{mode} , then

$$\begin{aligned}
& P(\#\{t \in \tilde{T}_{\text{II}}^+ \cap I_j^{\text{mode}} : y'_\gamma(t) - k(t) > u\} \geq 2) \\
&\leq P(\#\{t \in \tilde{T}_{\text{II}}^+ \cap I_j^{\text{mode}}\} \geq 2) \leq \exp\left(-\frac{a_j^2 D_{j,\gamma}^2}{2\sigma_3^2}\right).
\end{aligned}$$

Similarly, $P(\#\{t \in \tilde{T}_{\text{II}}^- \cap I_j^{\text{mode}} : y'_\gamma(t) - k(t) < -u\} \geq 2) \leq \exp\left(-\frac{a_j^2 D_{j,\gamma}^2}{2\sigma_3^2}\right)$.

On the other hand, since the probability that no local maxima of $y'_\gamma(t)$ in I_j^{mode} exceeding $u + k(t)$ is less than the probability that $y'_\gamma(t) - k(t) \leq u$ anywhere in I_j^{mode} , then

$$\begin{aligned}
& P(\#\{t \in \tilde{T}_{\text{II}}^+ \cap I_j^{\text{mode}} : y'_\gamma(t) - k(t) > u\} = 0) \\
&\leq P(y'_\gamma(t) - k(t) \leq u, \forall t \in I_j^{\text{mode}}) \\
&= P(z'_\gamma(t) + \mu'_\gamma(t) - k(t) \leq u, \forall t \in I_j^{\text{mode}}) \\
&\leq \Phi\left(\frac{u - a_j M_{j,\gamma}}{\sigma_1}\right) = \Phi\left(\frac{u - |a_j| M_{j,\gamma}}{\sigma_1}\right),
\end{aligned}$$

where the last line holds since $a_j > 0$ for $j \in \mathcal{I}_{\text{II}}^+$.

Therefore, the probability that only one local maximum of $y'_\gamma(t)$ in I_j^{mode} exceeds $u + k(t)$ is

$$\begin{aligned}
& P(\#\{t \in \tilde{T}_{\text{II}}^+ \cap I_j^{\text{mode}} : y'_\gamma(t) - k(t) > u\} = 1) \\
&= 1 - P(\#\{t \in \tilde{T}_{\text{II}}^+ \cap I_j^{\text{mode}} : y'_\gamma(t) - k(t) > u\} = 0) \\
&\quad - P(\#\{t \in \tilde{T}_{\text{II}}^+ \cap I_j^{\text{mode}} : y'_\gamma(t) - k(t) > u\} \geq 2) \quad (\text{C.39}) \\
&\geq 1 - \Phi\left(\frac{u - |a_j| M_{j,\gamma}}{\sigma_1}\right) - \exp\left(-\frac{a_j^2 D_{j,\gamma}^2}{2\sigma_3^2}\right).
\end{aligned}$$

The case of $j \in \mathcal{I}_{\text{II}}^-$ can be proved similarly. \square

Lemma S3. Let $\mathbb{T}_\gamma = \mathbb{S}_{1,\gamma} \setminus \mathbb{S}_1 = \cup_{j=1}^J (S_{j,\gamma} \setminus S_j)$ be the transition region. Let $W_{\mathbb{II},\gamma} = \#\{t \in \tilde{T}_{\mathbb{II}} \cap \mathbb{S}_{1,\gamma}\}$ and $W_{\mathbb{II},\gamma}(u) = \#\{t \in \tilde{T}_{\mathbb{II}}(u) \cap \mathbb{S}_{1,\gamma}\}$, where $W_{\mathbb{II},\gamma}(u) = W_{\mathbb{II},\gamma}^+(u) + W_{\mathbb{II},\gamma}^-(u) = \#\{t \in \tilde{T}_{\mathbb{II}}^+(u) \cap \mathbb{S}_{1,\gamma}\} + \#\{t \in \tilde{T}_{\mathbb{II}}^-(u) \cap \mathbb{S}_{1,\gamma}\}$. Then, under condition (C2), there exists $\eta > 0$ such that

(1). $P(\#\{t \in \tilde{T}_{\mathbb{II}} \cap \mathbb{T}_\gamma\} \geq 1) = o(\exp(-\eta a^2))$.

(2). $P(W_{\mathbb{II},\gamma} = J) = 1 - o(\exp(-\eta a^2))$.

(3). $P(W_{\mathbb{II},\gamma}(u) = J) = 1 - o(\exp(-\eta a^2))$.

(4). $W_{\mathbb{II},\gamma}/L = A + o_p(1)$.

(5). $W_{\mathbb{II},\gamma}(u)/W_{\mathbb{II},\gamma} = 1 + o_p(1)$.

Proof. (1). Note that $I_j^{\text{mode}} \subset S_j$ implies $T_{j,\gamma} \subset I_j^{\text{side}}$. Applying Lemma S2, we obtain

$$\begin{aligned} P(\#\{t \in \tilde{T}_{\mathbb{II}} \cap \mathbb{T}_\gamma\} \geq 1) &\leq P(\#\{t \in \tilde{T}_{\mathbb{II}} \cap (\cup_{j=1}^J I_j^{\text{side}})\} \geq 1) = P(\cup_{j=1}^J \#\{t \in \tilde{T}_{\mathbb{II}} \cap I_j^{\text{side}}\} \geq 1) \\ &\leq \sum_{j=1}^J [1 - P(\#\{t \in \tilde{T}_{\mathbb{II}} \cap I_j^{\text{side}}\} = 0)] \\ &\leq \sum_{j=1}^J \exp(-\frac{a_j^2 C_{j,\gamma}^2}{2\sigma_2^2}) \leq \sum_{j=1}^J \exp(-\frac{a^2 C_\gamma^2}{2\sigma_2^2}) \\ &= \frac{J}{L} L \exp(-\frac{a^2 C_\gamma^2}{2\sigma_2^2}) = o(\exp(-\eta a^2)), \end{aligned}$$

where $0 < \eta < C_\gamma^2/(2\sigma_2^2)$, and the last line holds because $J/L \rightarrow A$ and

$$L \exp(-\frac{a^2 C_\gamma^2}{2\sigma_2^2}) = \exp\{a^2(\frac{\log L}{a^2} - \frac{C_\gamma^2}{2\sigma_2^2})\} = o(\exp(-\eta a^2)) \text{ as } \frac{\log L}{a^2} \rightarrow 0.$$

(2). Applying Lemma S2, we have that there exists $\eta > 0$ such that

$$\begin{aligned}
P(W_{\text{II},\gamma} = J) &= P(\#\{t \in \tilde{T}_{\text{II}} \cap \mathbb{S}_{1,\gamma}\} = J) \\
&\geq P[\cap_{j=1}^J (\#\{t \in \tilde{T}_{\text{II}} \cap I_j^{\text{mode}}\} = 1 \cap \#\{t \in \tilde{T}_{\text{II}} \cap I_j^{\text{side}}\} = 0)] \\
&\geq 1 - \sum_{j=1}^J [1 - P(\#\{t \in \tilde{T}_{\text{II}} \cap I_j^{\text{mode}}\} = 1 \cap \#\{t \in \tilde{T}_{\text{II}} \cap I_j^{\text{side}}\} = 0)] \\
&\geq 1 - \sum_{j=1}^J [2 - P(\#\{t \in \tilde{T}_{\text{II}} \cap I_j^{\text{mode}}\} = 1) - P(\#\{t \in \tilde{T}_{\text{II}} \cap I_j^{\text{side}}\} = 0)] \\
&\geq 1 - \sum_{j=1}^J [2 - 2\Phi\left(\frac{|a_j|C_{j,\gamma}}{\sigma_2}\right) + \exp\left(-\frac{a_j^2 D_{j,\gamma}^2}{2\sigma_3^2}\right) + \exp\left(-\frac{a_j^2 C_{j,\gamma}^2}{2\sigma_2^2}\right)] \\
&\geq 1 - \frac{J}{L} \left\{ 2L \left[1 - \Phi\left(\frac{aC_\gamma}{\sigma_2}\right) \right] + L \exp\left(-\frac{a^2 C_\gamma^2}{2\sigma_2^2}\right) + L \exp\left(-\frac{a^2 D_\gamma^2}{2\sigma_3^2}\right) \right\} \\
&= 1 - o(\exp(-\eta a^2)),
\end{aligned}$$

where the last line holds because $L[1 - \Phi(Ka)] \leq L\phi(Ka)/(Ka)$ for any $K > 0$.

(3). Denote by $B_{j,0}$ and $B_{j,1}$ the events $\#\{t \in \tilde{T}_{\text{II}} \cap I_j^{\text{side}}\} = 0$ and $\#\{t \in \tilde{T}_{\text{II}}(u) \cap I_j^{\text{mode}}\} = 1$ respectively. Then, by Lemma S2, there exists $\eta > 0$ such that

$$\begin{aligned}
P(W_{\text{II},\gamma}(u) = J) &= P(W_{\text{II},\gamma}^+(u) + W_{\text{II},\gamma}^-(u) = J) \geq P(\cap_{j=1}^J (B_{j,0} \cap B_{j,1})) \\
&\geq 1 - \sum_{j=1}^J [1 - P(B_{j,0} \cap B_{j,1})] \\
&\geq 1 - \sum_{j=1}^J [1 - (P(B_{j,0}) + P(B_{j,1}) - 1)] \\
&\geq 1 - \sum_{j=1}^J \left[\exp\left(-a_j^2 \frac{D_{j,\gamma}^2}{2\sigma_3^2}\right) + \Phi\left(\frac{u - |a_j|M_{j,\gamma}}{\sigma_1}\right) + \exp\left(-a_j^2 \frac{C_{j,\gamma}^2}{2\sigma_2^2}\right) \right] \\
&\geq 1 - \sum_{j=1}^J \left[\exp\left(-a^2 \frac{D_\gamma^2}{2\sigma_3^2}\right) + \Phi\left(\frac{u - aM_\gamma}{\sigma_1}\right) + \exp\left(-a^2 \frac{C_\gamma^2}{2\sigma_2^2}\right) \right] \\
&= 1 - o(\exp(-\eta a^2)).
\end{aligned}$$

(4). It follows from part (2) that

$$\frac{W_{\text{II},\gamma}}{L} = \frac{W_{\text{II},\gamma}}{J} \frac{J}{L} = A(1 + o_p(1)) = A + o_p(1).$$

(5). Similarly to the proof of part (4), it follows from part (3) that $W_{\text{II},\gamma}(u)/L = A + o_p(1)$.

Then

$$W_{\text{II},\gamma}(u)/W_{\text{II},\gamma} = (W_{\text{II},\gamma}(u)/L)/(W_{\text{II},\gamma}/L) = 1 + o_p(1).$$

□

D FDR Control and Power Consistency for Type II Change Points

D.1 FDR control

Proof of Theorem 2 (FDR control). Recall that $V_{\text{II}}(u) = \#\{t \in \tilde{T}_{\text{II}}(u) \cap \mathbb{S}_0\}$ and $W_{\text{II},\gamma}(u) = \#\{t \in \tilde{T}_{\text{II}}(u) \cap \mathbb{S}_{1,\gamma}\}$. Let $W_{\text{II}}(u) = \#\{t \in \tilde{T}_{\text{II}}(u) \cap \mathbb{S}_1\}$ and $V_{\text{II},\gamma}(u) = \#\{t \in \tilde{T}_{\text{II}}(u) \cap \mathbb{S}_{0,\gamma}\}$. That is, $V_{\text{II}}(u)$ and $W_{\text{II}}(u)$ represent the number of local maxima above u plus local minima below $-u$ in the *null region* and *signal region* respectively; and $V_{\text{II},\gamma}(u)$ and $W_{\text{II},\gamma}(u)$ represent the number of local maxima above u plus local minima below $-u$ in the *smoothed null region* and *smoothed signal region* respectively. Accordingly, V_{II} , W_{II} , $V_{\text{II},\gamma}$ and $W_{\text{II},\gamma}$ are defined as the number of extrema in \mathbb{S}_0 , \mathbb{S}_1 , $\mathbb{S}_{0,\gamma}$, $\mathbb{S}_{1,\gamma}$, respectively. Note that $R_{\text{II}}(u) = \#\{t \in \tilde{T}_{\text{II}}(u)\} = V_{\text{II}}(u) + W_{\text{II}}(u)$. By the definition of FDR for Type II change points detection, for any fixed u , we have

$$\text{FDR}_{\text{II}}(u) = E\left[\frac{V_{\text{II}}(u)}{V_{\text{II}}(u) + W_{\text{II}}(u)}\right] = E\left[\frac{V_{\text{II}}(u)/L}{V_{\text{II}}(u)/L + W_{\text{II}}(u)/L}\right]. \quad (\text{D.40})$$

Note that

$$\begin{aligned} P(V_{\text{II},\gamma}(u) = V_{\text{II}}(u)) &= 1 - P(V_{\text{II},\gamma}(u) \neq V_{\text{II}}(u)) = 1 - P(\#\{t \in \tilde{T}_{\text{II}}(u) \cap \mathbb{T}_\gamma\} \geq 1) \\ &\geq 1 - P(\#\{t \in \tilde{T}_{\text{II}} \cap \mathbb{T}_\gamma\} \geq 1) = 1 - o(\exp(-\eta a^2)) \rightarrow 1. \end{aligned}$$

Hence, $V_{\text{II},\gamma}(u) = V_{\text{II}}(u) + o_p(1)$. Similarly, we have $W_{\text{II},\gamma}(u) = W_{\text{II}}(u) + o_p(1)$.

Then it follows that

$$\begin{aligned} \frac{V_{\text{II}}(u)}{L} &= \frac{V_{\text{II}}(u)}{V_{\text{II},\gamma}(u)} \frac{V_{\text{II},\gamma}(u)}{L} = [1 + o_p(1)] \frac{[L - J(2c\gamma)]E[\tilde{m}_{z'_\gamma}(U(1), u)]}{L} \\ &= (1 - 2c\gamma A)E[\tilde{m}_{z'_\gamma}(U(1), u)] + o_p(1), \\ \frac{W_{\text{II}}(u)}{L} &= \frac{W_{\text{II}}(u)}{W_{\text{II},\gamma}(u)} \frac{W_{\text{II},\gamma}(u)}{L} = [1 + o_p(1)][A + o_p(1)] = A + o_p(1). \end{aligned}$$

Hence,

$$\frac{V_{\Pi}(u)/L}{V_{\Pi}(u)/L + W_{\Pi}(u)/L} = \frac{(1 - 2c\gamma A)E[\tilde{m}_{z'_\gamma}(U(1), u)]}{A + (1 - 2c\gamma A)E[\tilde{m}_{z'_\gamma}(U(1), u)]} + o_p(1) < 1. \quad (\text{D.41})$$

As $\frac{V_{\Pi}(u)}{V_{\Pi}(u) + W_{\Pi}(u)} \leq 1$, by the Dominated Convergence Theorem (DCT),

$$\begin{aligned} \lim E\left[\frac{V_{\Pi}(u)/L}{V_{\Pi}(u)/L + W_{\Pi}(u)/L}\right] &= E\left[\lim \frac{V_{\Pi}(u)/L}{V_{\Pi}(u)/L + W_{\Pi}(u)/L}\right] \\ &= \frac{(1 - 2c\gamma A)E[\tilde{m}_{z'_\gamma}(U(1), u)]}{A + (1 - 2c\gamma A)E[\tilde{m}_{z'_\gamma}(U(1), u)]}. \end{aligned}$$

That is,

$$\text{FDR}_{\Pi}(u) \rightarrow \frac{(1 - 2c\gamma A)E[\tilde{m}_{z'_\gamma}(U(1), u)]}{A + (1 - 2c\gamma A)E[\tilde{m}_{z'_\gamma}(U(1), u)]}, \quad (\text{D.42})$$

completing Part (i) in Theorem 2 for the FDR control.

Next we will show the FDR control for random threshold \tilde{u}_{Π} . Let $\tilde{G}(u) = \#\{t \in \tilde{T}_{\Pi}(u)\} / \#\{t \in \tilde{T}_{\Pi}\}$ be the empirical marginal right cdf of $z'_\gamma(t)$ given $t \in \tilde{T}_{\Pi}$. By the Benjamini-Hochberg (BH) procedure, the BH threshold \tilde{u}_{Π} satisfies $\alpha \tilde{G}(\tilde{u}_{\Pi}) = k\alpha / m_{\Pi} = F_{z'_\gamma}(\tilde{u}_{\Pi})$, so \tilde{u}_{Π} is the largest u that solves the equation

$$\alpha \tilde{G}(u) = F_{z'_\gamma}(u). \quad (\text{D.43})$$

Note that

$$\tilde{G}(u) = \frac{V_{\Pi,\gamma}(u) + W_{\Pi,\gamma}(u)}{V_{\Pi,\gamma} + W_{\Pi,\gamma}} = \frac{V_{\Pi,\gamma}(u)}{V_{\Pi,\gamma}} \frac{V_{\Pi,\gamma}}{V_{\Pi,\gamma} + W_{\Pi,\gamma}} + \frac{W_{\Pi,\gamma}(u)}{W_{\Pi,\gamma}} \frac{W_{\Pi,\gamma}}{V_{\Pi,\gamma} + W_{\Pi,\gamma}},$$

By the weak law of large numbers or Lemma 8 in [Schwartzman et al. \(2011\)](#),

$$\frac{V_{\Pi,\gamma}(u)/L}{V_{\Pi,\gamma}/L} \xrightarrow{P} \frac{E[V_{\Pi,\gamma}(u)]}{E[V_{\Pi,\gamma}]} = F_{z'_\gamma}(u). \quad (\text{D.44})$$

In addition,

$$\frac{V_{\Pi,\gamma}}{V_{\Pi,\gamma} + W_{\Pi,\gamma}} = \frac{V_{\Pi,\gamma}/L}{V_{\Pi,\gamma}/L + W_{\Pi,\gamma}/L} \xrightarrow{P} \frac{E[\tilde{m}_{z'_\gamma}(U(1))](1 - 2c\gamma A)}{E[\tilde{m}_{z'_\gamma}(U(1))](1 - 2c\gamma A) + A},$$

and

$$\frac{W_{\Pi,\gamma}}{V_{\Pi,\gamma} + W_{\Pi,\gamma}} = \frac{W_{\Pi,\gamma}/L}{V_{\Pi,\gamma}/L + W_{\Pi,\gamma}/L} \xrightarrow{P} \frac{A}{E[\tilde{m}_{z'_\gamma}(U(1))](1 - 2c\gamma A) + A}.$$

Combining these with (D.43) and Part (5) in Lemma S3, we obtain

$$\tilde{G}(u) \xrightarrow{P} F_{z'_\gamma}(u) \frac{E[\tilde{m}_{z'_\gamma}(U(1))](1 - 2c\gamma A)}{E[\tilde{m}_{z'_\gamma}(U(1))](1 - 2c\gamma A) + A} + \frac{A}{E[\tilde{m}_{z'_\gamma}(U(1))](1 - 2c\gamma A) + A}.$$

Plugging $\tilde{G}(u)$ by this limit in (D.43) and solving for u gives the deterministic solution u_{Π}^* such that

$$F_{z'_\gamma}(u_{\Pi}^*) = \frac{\alpha A}{A + E[\tilde{m}_{z'_\gamma}(U(1))](1 - 2c\gamma A)(1 - \alpha)}. \quad (\text{D.45})$$

Note that \tilde{u}_{Π} is the solution of $\alpha\tilde{G}(u) = F_{z'_\gamma}(u)$ and u_{Π}^* is the solution of $\lim \alpha\tilde{G}(u) = F_{z'_\gamma}(u)$, and since $F_{z'_\gamma}^{-1}(\cdot)$ is continuous and monotonic, we have $\tilde{u}_{\Pi} \xrightarrow{P} u_{\Pi}^*$. That is, for any $\epsilon > 0$,

$$P(|\tilde{u}_{\Pi} - u_{\Pi}^*| > \epsilon) \rightarrow 0.$$

By the definition of FDR, for the random threshold \tilde{u}_{Π} and $\epsilon > 0$,

$$\begin{aligned} \text{FDR}_{\Pi, \text{BH}} &= \text{FDR}_{\Pi}(\tilde{u}_{\Pi}) = E\left[\frac{V_{\Pi}(\tilde{u}_{\Pi})}{V_{\Pi}(\tilde{u}_{\Pi}) + W_{\Pi}(\tilde{u}_{\Pi})}\right] \\ &= E\left[\frac{V_{\Pi}(\tilde{u}_{\Pi})}{V_{\Pi}(\tilde{u}_{\Pi}) + W_{\Pi}(\tilde{u}_{\Pi})} \mathbb{1}(|\tilde{u}_{\Pi} - u_{\Pi}^*| \leq \epsilon)\right] + E\left[\frac{V_{\Pi}(\tilde{u}_{\Pi})}{V_{\Pi}(\tilde{u}_{\Pi}) + W_{\Pi}(\tilde{u}_{\Pi})} \mathbb{1}(|\tilde{u}_{\Pi} - u_{\Pi}^*| > \epsilon)\right] \\ &= E\left[\frac{V_{\Pi}(\tilde{u}_{\Pi})}{V_{\Pi}(\tilde{u}_{\Pi}) + W_{\Pi}(\tilde{u}_{\Pi})} \mathbb{1}(|\tilde{u}_{\Pi} - u_{\Pi}^*| \leq \epsilon)\right] + o(1). \end{aligned} \quad (\text{D.46})$$

Since both $V_{\Pi}(u)$ and $W_{\Pi}(u)$ are decreasing with respect to u , we have that, for L large enough,

$$\begin{aligned} E\left[\frac{V_{\Pi}(\tilde{u}_{\Pi})}{V_{\Pi}(\tilde{u}_{\Pi}) + W_{\Pi}(\tilde{u}_{\Pi})} \mathbb{1}(|\tilde{u}_{\Pi} - u_{\Pi}^*| \leq \epsilon)\right] &\geq E\left[\frac{V_{\Pi}(u_{\Pi}^* + \epsilon)}{V_{\Pi}(u_{\Pi}^* - \epsilon) + W_{\Pi}(u_{\Pi}^* - \epsilon)} \mathbb{1}(|\tilde{u}_{\Pi} - u_{\Pi}^*| \leq \epsilon)\right], \\ E\left[\frac{V_{\Pi}(\tilde{u}_{\Pi})}{V_{\Pi}(\tilde{u}_{\Pi}) + W_{\Pi}(\tilde{u}_{\Pi})} \mathbb{1}(|\tilde{u}_{\Pi} - u_{\Pi}^*| \leq \epsilon)\right] &\leq E\left[\frac{V_{\Pi}(u_{\Pi}^* - \epsilon)}{V_{\Pi}(u_{\Pi}^* + \epsilon) + W_{\Pi}(u_{\Pi}^* + \epsilon)}\right]. \end{aligned}$$

Additionally, note that the expectation of the number of extrema exceeding level u is continuous in u by the Kac-Rice formula. Thus, similarly to (D.41), we have that, for large L , as $\epsilon \rightarrow 0$,

$$\begin{aligned} &\left| E\left[\frac{V_{\Pi}(u_{\Pi}^* + \epsilon)}{V_{\Pi}(u_{\Pi}^* - \epsilon) + W_{\Pi}(u_{\Pi}^* - \epsilon)} \mathbb{1}(|\tilde{u}_{\Pi} - u_{\Pi}^*| \leq \epsilon)\right] - E\left[\frac{V_{\Pi}(u_{\Pi}^*)}{V_{\Pi}(u_{\Pi}^*) + W_{\Pi}(u_{\Pi}^*)}\right] \right| \\ &\leq \left| E\left[\frac{V_{\Pi}(u_{\Pi}^* + \epsilon)}{V_{\Pi}(u_{\Pi}^* - \epsilon) + W_{\Pi}(u_{\Pi}^* - \epsilon)} \mathbb{1}(|\tilde{u}_{\Pi} - u_{\Pi}^*| \leq \epsilon)\right] - E\left[\frac{V_{\Pi}(u_{\Pi}^* + \epsilon)}{V_{\Pi}(u_{\Pi}^* - \epsilon) + W_{\Pi}(u_{\Pi}^* - \epsilon)}\right] \right| \\ &\quad + \left| E\left[\frac{V_{\Pi}(u_{\Pi}^* + \epsilon)/L}{V_{\Pi}(u_{\Pi}^* - \epsilon)/L + W_{\Pi}(u_{\Pi}^* - \epsilon)/L}\right] - E\left[\frac{V_{\Pi}(u_{\Pi}^*)/L}{V_{\Pi}(u_{\Pi}^*)/L + W_{\Pi}(u_{\Pi}^*)/L}\right] \right| \\ &\rightarrow 0 \end{aligned}$$

and

$$\left| E\left[\frac{V_{\Pi}(u_{\Pi}^* - \epsilon)}{V_{\Pi}(u_{\Pi}^* + \epsilon) + W_{\Pi}(u_{\Pi}^* + \epsilon)}\right] - E\left[\frac{V_{\Pi}(u_{\Pi}^*)}{V_{\Pi}(u_{\Pi}^*) + W_{\Pi}(u_{\Pi}^*)}\right] \right| \rightarrow 0,$$

which implies

$$E\left[\frac{V_{\Pi}(\tilde{u}_{\Pi})}{V_{\Pi}(\tilde{u}_{\Pi}) + W_{\Pi}(\tilde{u}_{\Pi})} \mathbb{1}(|\tilde{u}_{\Pi} - u_{\Pi}^*| \leq \epsilon)\right] - E\left[\frac{V_{\Pi}(u_{\Pi}^*)}{V_{\Pi}(u_{\Pi}^*) + W_{\Pi}(u_{\Pi}^*)}\right] \rightarrow 0. \quad (\text{D.47})$$

Therefore, by (D.46) and (D.47), we obtain

$$\begin{aligned} \lim \text{FDR}_{\Pi, \text{BH}} &= \lim E\left[\frac{V_{\Pi}(\tilde{u}_{\Pi})}{V_{\Pi}(\tilde{u}_{\Pi}) + W_{\Pi}(\tilde{u}_{\Pi})} \mathbb{1}(|\tilde{u}_{\Pi} - u_{\Pi}^*| \leq \epsilon)\right] \\ &= \lim E\left[\frac{V_{\Pi}(u_{\Pi}^*)}{V_{\Pi}(u_{\Pi}^*) + W_{\Pi}(u_{\Pi}^*)}\right] \\ &= E\left[\lim \frac{V_{\Pi}(u_{\Pi}^*)/L}{V_{\Pi}(u_{\Pi}^*)/L + W_{\Pi}(u_{\Pi}^*)/L}\right] \\ &= \frac{F_{z_{\gamma}'}(u_{\Pi}^*)E[\tilde{m}_{z_{\gamma}'}(U(1))](1 - 2c\gamma A)}{F_{z_{\gamma}'}(u_{\Pi}^*)E[\tilde{m}_{z_{\gamma}'}(U(1))](1 - 2c\gamma A) + A} \quad (\text{by (D.41) and (D.44)}) \\ &= \alpha \frac{E[\tilde{m}_{z_{\gamma}'}(U(1))](1 - 2c\gamma A)}{E[\tilde{m}_{z_{\gamma}'}(U(1))](1 - 2c\gamma A) + A} \quad (\text{by (D.45)}). \end{aligned} \quad (\text{D.48})$$

□

D.2 Power consistency

Proof of Theorem 2 (power consistency). By Lemma S2, for any fixed u ,

$$\begin{aligned} \text{Power}_{\Pi, j}(u) &= P(\#\{t \in \tilde{T}_{\Pi}(u) \cap S_j\} \geq 1) \\ &\geq P(\#\{t \in \tilde{T}_{\Pi}(u) \cap I_j^{\text{mode}}\} \geq 1) \\ &\geq 1 - \exp\left(-\frac{a_j^2 D_{j, \gamma}^2}{2\sigma^3}\right) - \Phi\left(\frac{u - |a_j| M_{j, \gamma}}{\sigma_1}\right) \rightarrow 1. \end{aligned}$$

Therefore,

$$\text{Power}_{\Pi}(u) = \frac{1}{J} \sum_{j=1}^J \text{Power}_{\Pi, j}(u) \rightarrow 1.$$

For the random threshold \tilde{u}_{Π} and arbitrary $\epsilon > 0$, we have

$$\begin{aligned} P(\#\{t \in \tilde{T}_{\Pi}(\tilde{u}_{\Pi}) \cap S_j\} \geq 1) &= P(\#\{t \in \tilde{T}_{\Pi}(\tilde{u}_{\Pi}) \cap S_j\} \geq 1, |\tilde{u}_{\Pi} - u_{\Pi}^*| \leq \epsilon) \\ &\quad + P(\#\{t \in \tilde{T}_{\Pi}(\tilde{u}_{\Pi}) \cap S_j\} \geq 1, |\tilde{u}_{\Pi} - u_{\Pi}^*| > \epsilon), \end{aligned} \quad (\text{D.49})$$

where the last term is bounded above by $P(|\tilde{u}_{\text{II}} - u_{\text{II}}^*| > \epsilon) \rightarrow 0$ as $\epsilon \rightarrow 0$. Moreover,

$$\begin{aligned} & P(\#\{t \in \tilde{T}_{\text{II}}(\tilde{u}_{\text{II}}) \cap S_j\} \geq 1, |\tilde{u}_{\text{II}} - u_{\text{II}}^*| \leq \epsilon) \\ & \geq P(\#\{t \in \tilde{T}_{\text{II}}(u_{\text{II}}^* + \epsilon) \cap S_j\} \geq 1, |\tilde{u}_{\text{II}} - u_{\text{II}}^*| \leq \epsilon) \\ & \geq 1 - P(\#\{t \in \tilde{T}_{\text{II}}(u_{\text{II}}^* + \epsilon) \cap S_j\} = 0) - P(|\tilde{u}_{\text{II}} - u_{\text{II}}^*| > \epsilon) \rightarrow 1, \end{aligned}$$

where the last line holds because for any two events A and B , $P(A \cap B) = 1 - P(A^c \cup B^c) \geq 1 - P(A^c) - P(B^c)$. Therefore, by Lemma S2, $\text{Power}_{\text{II},j}(\tilde{u}_{\text{II}}) \rightarrow 1$, and hence

$$\text{Power}_{\text{II},\text{BH}} = \text{Power}_{\text{II},\text{BH}}(\tilde{u}_{\text{II}}) = \frac{1}{J} \sum_{j=1}^J \text{Power}_{\text{II},j}(\tilde{u}_{\text{II}}) \rightarrow 1.$$

□

E FDR Control and Power Consistency for Mixture of Type I and Type II Change Points

E.1 FDR control

Proof of Theorem 3 (FDR control). Recall that the FDR for mixture of Type I and Type II change points is defined as

$$\text{FDR}_{\text{III}}(u_1, u_2) = E \left\{ \frac{V_{\text{I}\setminus\text{II}}(u_1) + V_{\text{II}}(u_2)}{R_{\text{I}\setminus\text{II}}(u_1) + R_{\text{II}}(u_2)} \right\},$$

and that $\mathbb{S}_{1,\text{I}\setminus\text{II}} = \cup_{j=1}^{J_1} (v_j - b, v_j + b) \setminus \mathbb{S}_{\text{II}}^*$, where v_j is a Type I change point and $\mathbb{S}_{\text{II}}^* = \cup_{i=1}^{R_{\text{II}}(u_2)} (\hat{v}_i - 2\gamma, \hat{v}_i + 2\gamma)$ for all significant $\hat{v}_i \in \tilde{T}_{\text{II}}$. Let $\mathbb{S}_{1,\gamma,\text{I}\setminus\text{II}}$ and $\mathbb{S}_{0,\gamma,\text{I}\setminus\text{II}}$ be the smoothed signal region and smoothed null region of Type I change points, denoted by $\mathbb{S}_{1,\gamma,\text{I}\setminus\text{II}} = \cup_{j=1}^{J_1} (v_j - c\gamma, v_j + c\gamma) \setminus \mathbb{S}_{\text{II}}^*$ and $\mathbb{S}_{0,\gamma,\text{I}\setminus\text{II}} = U(L) \setminus \mathbb{S}_{1,\gamma,\text{I}\setminus\text{II}}$.

Let $W_{\text{I}\setminus\text{II}}(u_1) = \#\{t \in \tilde{T}_{\text{I}\setminus\text{II}}(u_1) \cap \mathbb{S}_{1,\text{I}\setminus\text{II}}\}$ and $W_{\text{I}\setminus\text{II},\gamma}(u_1) = \#\{t \in \tilde{T}_{\text{I}\setminus\text{II}}(u_1) \cap \mathbb{S}_{1,\gamma,\text{I}\setminus\text{II}}\}$.

Then $R_{\text{I}\setminus\text{II}}(u_1) = V_{\text{I}\setminus\text{II}}(u_1) + W_{\text{I}\setminus\text{II}}(u_1)$, and $\text{FDR}_{\text{III}}(u_1, u_2)$ can be rewritten as

$$\begin{aligned} \text{FDR}_{\text{III}}(u_1, u_2) &= E \left[\frac{V_{\text{I}\setminus\text{II}}(u_1) + V_{\text{II}}(u_2)}{V_{\text{I}\setminus\text{II}}(u_1) + W_{\text{I}\setminus\text{II}}(u_1) + V_{\text{II}}(u_2) + W_{\text{II}}(u_2)} \right] \\ &= E \left\{ E \left[\frac{V_{\text{I}\setminus\text{II}}(u_1) + V_{\text{II}}(u_2)}{V_{\text{I}\setminus\text{II}}(u_1) + W_{\text{I}\setminus\text{II}}(u_1) + V_{\text{II}}(u_2) + W_{\text{II}}(u_2)} \middle| V_{\text{II}}(u_2) \right] \right\} \end{aligned}$$

Let $\Delta(u_2)$ be the length of $\mathbb{S}_{0,\gamma,I\setminus\Pi}$. Then

$$L - 2c\gamma J_1 - 4\gamma R_{\Pi}(u_2) \leq \Delta(u_2) \leq L - 2c\gamma J_1,$$

where the left inequality holds because some of the falsely detected Type II change points may overlap with Type I change points.

Recall that for the detection of Type II change points in step 1 of Algorithm 3, we have

$$\begin{aligned} \frac{V_{\Pi}(u_2)}{L} &\rightarrow E[\tilde{m}_{z'_\gamma}(U(1), u_2)](1 - 2c\gamma A_2), \\ \frac{W_{\Pi}(u_2)}{L} &\rightarrow A_2. \end{aligned}$$

Since we assume that the distance between neighboring change points are large enough, and the detected Type II change points have been removed when detecting Type I change points, then $V_{I\setminus\Pi}(u_1)$ and $W_{I\setminus\Pi}(u_1)$ only depend on $V_{\Pi}(u_2)$,

$$\begin{aligned} \frac{V_{I\setminus\Pi}(u_1)}{L} \Big| V_{\Pi}(u_2) &\sim E[\tilde{m}_{z''_\gamma}(U(1), u_1)]\Delta(u_2)/L, \\ \frac{W_{I\setminus\Pi}(u_1)}{L} \Big| V_{\Pi}(u_2) &= \frac{W_{I\setminus\Pi}(u_1)}{W_{I\setminus\Pi,\gamma}(u_1)} \frac{W_{I\setminus\Pi,\gamma}(u_1)}{L} = \frac{W_{I\setminus\Pi,\gamma}(u_1)}{L} + o_p(1). \end{aligned}$$

Moreover, notice that the falsely detected Type II change points mainly result from random noise (due to FDR control), which are uniformly distributed over the null signal region of Type I change points. Hence in fact, $\cup_{j=1}^{J_1} (v_j - c\gamma, v_j + c\gamma) \cap \mathbb{S}_{\Pi}^*$ tends to an empty set. Thus $\frac{W_{I\setminus\Pi,\gamma}(u_1)}{L} \rightarrow A_1$ and

$$\begin{aligned} &\frac{V_{I\setminus\Pi}(u_1) + V_{\Pi}(u_2)}{V_{I\setminus\Pi}(u_1) + W_{I\setminus\Pi}(u_1) + V_{\Pi}(u_2) + W_{\Pi}(u_2)} \Big| V_{\Pi}(u_2) \\ &= \frac{V_{I\setminus\Pi}(u_1)/L + V_{\Pi}(u_2)/L}{V_{I\setminus\Pi}(u_1)/L + W_{I\setminus\Pi}(u_1)/L + V_{\Pi}(u_2)/L + W_{\Pi}(u_2)/L} \Big| V_{\Pi}(u_2) \\ &\sim \frac{E[\tilde{m}_{z''_\gamma}(U(1), u_1)]\Delta(u_2)/L + V_{\Pi}(u_2)/L}{E[\tilde{m}_{z''_\gamma}(U(1), u_1)]\Delta(u_2)/L + V_{\Pi}(u_2)/L + A_1 + A_2} \Big| V_{\Pi}(u_2). \end{aligned}$$

As $\Delta(u_2) \leq L - 2c\gamma J_1$, by DCT, we obtain

$$\begin{aligned}
\lim \text{FDR}_{\text{III}}(u_1, u_2) &= \lim E\left\{E\left[\frac{V_{\text{I}\setminus\text{II}}(u_1) + V_{\text{II}}(u_2)}{V_{\text{I}\setminus\text{II}}(u_1) + W_{\text{I}\setminus\text{II}}(u_1) + V_{\text{II}}(u_2) + W_{\text{II}}(u_2)} \middle| V_{\text{II}}(u_2)\right]\right\} \\
&= E\left\{\lim E\left[\frac{V_{\text{I}\setminus\text{II}}(u_1)/L + V_{\text{II}}(u_2)/L}{V_{\text{I}\setminus\text{II}}(u_1)/L + W_{\text{I}\setminus\text{II}}(u_1)/L + V_{\text{II}}(u_2)/L + W_{\text{II}}(u_2)/L} \middle| V_{\text{II}}(u_2)\right]\right\} \quad (\text{E.50}) \\
&\leq \frac{E[\tilde{m}_{z_\gamma''}(U(1), u_1)](1 - 2c\gamma A_1) + E[\tilde{m}_{z_\gamma'}(U(1), u_2)](1 - 2c\gamma A_2)}{E[\tilde{m}_{z_\gamma''}(U(1), u_1)](1 - 2c\gamma A_1) + E[\tilde{m}_{z_\gamma'}(U(1), u_2)](1 - 2c\gamma A_2) + A}.
\end{aligned}$$

For the random thresholds \tilde{u}_{I} and \tilde{u}_{II} ,

$$\begin{aligned}
\text{FDR}_{\text{III}}(\tilde{u}_{\text{I}}, \tilde{u}_{\text{II}}) &= E\left[\frac{V_{\text{I}\setminus\text{II}}(\tilde{u}_{\text{I}}) + V_{\text{II}}(\tilde{u}_{\text{II}})}{V_{\text{I}\setminus\text{II}}(\tilde{u}_{\text{I}}) + W_{\text{I}\setminus\text{II}}(\tilde{u}_{\text{I}}) + V_{\text{II}}(\tilde{u}_{\text{II}}) + W_{\text{II}}(\tilde{u}_{\text{II}})}\right] \\
&= E\left\{E\left[\frac{V_{\text{I}\setminus\text{II}}(\tilde{u}_{\text{I}}) + V_{\text{II}}(\tilde{u}_{\text{II}})}{V_{\text{I}\setminus\text{II}}(\tilde{u}_{\text{I}}) + W_{\text{I}\setminus\text{II}}(\tilde{u}_{\text{I}}) + V_{\text{II}}(\tilde{u}_{\text{II}}) + W_{\text{II}}(\tilde{u}_{\text{II}})} \middle| V_{\text{II}}(\tilde{u}_{\text{II}})\right]\right\}.
\end{aligned}$$

Similarly to (D.48), we obtain that, as $\tilde{u}_{\text{I}} \xrightarrow{P} u_{\text{I}}^*$,

$$\text{FDR}_{\text{III}}(\tilde{u}_{\text{I}}, \tilde{u}_{\text{II}}) \sim E\left[\frac{V_{\text{II}}(\tilde{u}_{\text{II}})/L + F_{z_\gamma''}(u_{\text{I}}^*)E[\tilde{m}_{z_\gamma''}(U(1))]\Delta(\tilde{u}_{\text{II}})/L}{V_{\text{II}}(\tilde{u}_{\text{II}})/L + W_{\text{II}}(\tilde{u}_{\text{II}})/L + F_{z_\gamma''}(u_{\text{I}}^*)E[\tilde{m}_{z_\gamma''}(U(1))]\Delta(\tilde{u}_{\text{II}})/L + A_1}\right],$$

where

$$L - 2c\gamma J_1 - 4\gamma R_{\text{II}}(\tilde{u}_{\text{II}}) \leq \Delta(\tilde{u}_{\text{II}}) \leq L - 2c\gamma J_1,$$

$$F_{z_\gamma''}(u_{\text{I}}^*) = \frac{\alpha A_1}{A_1 + (1 - \alpha)E[\tilde{m}_{z_\gamma''}(U(1))]\Delta(\tilde{u}_{\text{II}})/L}.$$

Additionally,

$$\begin{aligned}
F_{z_\gamma''}(u_{\text{I}}^*)\Delta(\tilde{u}_{\text{II}})/L &= \frac{\alpha A_1 \Delta(\tilde{u}_{\text{II}})/L}{A_1 + (1 - \alpha)E[\tilde{m}_{z_\gamma''}(U(1))]\Delta(\tilde{u}_{\text{II}})/L} \\
&\leq \frac{\alpha A_1 (1 - 2c\gamma A_1)}{A_1 + (1 - \alpha)E[\tilde{m}_{z_\gamma''}(U(1))](1 - 2c\gamma A_1)}.
\end{aligned}$$

Therefore,

$$\begin{aligned}
&\lim \text{FDR}_{\text{III}}(\tilde{u}_{\text{I}}, \tilde{u}_{\text{II}}) \\
&= E\left[\lim \frac{V_{\text{II}}(\tilde{u}_{\text{II}})/L + F_{z_\gamma''}(u_{\text{I}}^*)E[\tilde{m}_{z_\gamma''}(U(1))]\Delta(\tilde{u}_{\text{II}})/L}{V_{\text{II}}(\tilde{u}_{\text{II}})/L + W_{\text{II}}(\tilde{u}_{\text{II}})/L + F_{z_\gamma''}(u_{\text{I}}^*)E[\tilde{m}_{z_\gamma''}(U(1))]\Delta(\tilde{u}_{\text{II}})/L + \tilde{A}_1^*}\right] \\
&\leq E\left[\lim \frac{V_{\text{II}}(\tilde{u}_{\text{II}})/L + E[\tilde{m}_{z_\gamma''}(U(1))]\frac{\alpha A_1 (1 - 2c\gamma A_1)}{A_1 + (1 - \alpha)E[\tilde{m}_{z_\gamma''}(U(1))](1 - 2c\gamma A_1)}}{V_{\text{II}}(\tilde{u}_{\text{II}})/L + W_{\text{II}}(\tilde{u}_{\text{II}})/L + A_1 + E[\tilde{m}_{z_\gamma''}(U(1))]\frac{\alpha A_1 (1 - 2c\gamma A_1)}{A_1 + (1 - \alpha)E[\tilde{m}_{z_\gamma''}(U(1))](1 - 2c\gamma A_1)}}\right] \\
&= E\left[\lim \frac{V_{\text{II}}(u_{\text{II}}^*)/L + E[\tilde{m}_{z_\gamma''}(U(1))]\frac{\alpha A_1 (1 - 2c\gamma A_1)}{A_1 + (1 - \alpha)E[\tilde{m}_{z_\gamma''}(U(1))](1 - 2c\gamma A_1)}}{V_{\text{II}}(u_{\text{II}}^*)/L + W_{\text{II}}(u_{\text{II}}^*)/L + A_1 + E[\tilde{m}_{z_\gamma''}(U(1))]\frac{\alpha A_1 (1 - 2c\gamma A_1)}{A_1 + (1 - \alpha)E[\tilde{m}_{z_\gamma''}(U(1))](1 - 2c\gamma A_1)}}\right] \\
&\leq \alpha,
\end{aligned}$$

where the last line holds because by (D.48),

$$E\left[\lim \frac{V_{\text{II}}(u_{\text{II}}^*)/L}{V_{\text{II}}(u_{\text{II}}^*)/L + A_2}\right] \leq \alpha,$$

and on the other hand,

$$\begin{aligned} & \frac{E[\tilde{m}_{z\gamma}''(U(1))]}{A_1 + (1-\alpha)E[\tilde{m}_{z\gamma}''(U(1))]} \frac{\alpha A_1(1-2c\gamma A_1)}{(1-2c\gamma A_1)} \\ & \frac{A_1 + E[\tilde{m}_{z\gamma}''(U(1))]}{A_1 + (1-\alpha)E[\tilde{m}_{z\gamma}''(U(1))]} \frac{\alpha A_1(1-2c\gamma A_1)}{(1-2c\gamma A_1)} \\ & = \alpha \frac{(1-2c\gamma A_1)E[\tilde{m}_{z\gamma}''(U(1))]}{A_1 + (1-2c\gamma A_1)E[\tilde{m}_{z\gamma}''(U(1))]} \leq \alpha. \end{aligned}$$

Here we have used an evident fact that $(a_1 + a_2)/(b_1 + b_2) \leq \alpha$ if $a_1/b_1 \leq \alpha$, $a_2/b_2 \leq \alpha$ and $b_1 > 0, b_2 > 0$. \square

E.2 Power consistency

Proof of Theorem 3 (power consistency). Recall that, if v_j is a Type II break, then $\text{Power}_{\text{II},j}(u_2) = P(\#\{t \in \tilde{T}_{\text{II}}(u_2) \cap S_j\} \geq 1)$; and if v_j is a Type I break, then $\text{Power}_{\text{I},j}(u_1) = P(\#\{t \in \tilde{T}_{\text{I}}(u_1) \cap S_j\} \geq 1)$. It is shown in the proofs of Theorems 1 and 2 that, for each j , both $\text{Power}_{\text{I},j}(u_1)$ and $\text{Power}_{\text{II},j}(u_2)$ tend to 1 as $L \rightarrow \infty$. Therefore, we obtain

$$\text{Power}_{\text{III}}(u_1, u_2) = \frac{1}{J} \sum_{j=1}^J \left[\text{Power}_{\text{I},j}(u_1) \mathbb{1}(v_j \text{ is Type I}) + \text{Power}_{\text{II},j}(u_2) \mathbb{1}(v_j \text{ is Type II}) \right] \rightarrow 1.$$

Similarly to the proofs of power consistency in Theorems 1 and 2, for the random thresholds \tilde{u}_{I} and \tilde{u}_{II} , we have that, if v_j is a Type I break, then $\text{Power}_{\text{I},j}(\tilde{u}_{\text{I}}) \rightarrow 1$; and if v_j is a Type II break, then $\text{Power}_{\text{II},j}(\tilde{u}_{\text{II}}) \rightarrow 1$. Thus,

$$\text{Power}_{\text{III,BH}} = \text{Power}_{\text{III}}(\tilde{u}_{\text{I}}, \tilde{u}_{\text{II}}) \rightarrow 1.$$

\square

References

- Andrews, D. W. (1993), 'Tests for parameter instability and structural change with unknown change point', *Econometrica: Journal of the Econometric Society* pp. 821–856.
- Andrews, D. W., Lee, I. and Ploberger, W. (1996), 'Optimal changepoint tests for normal linear regression', *Journal of Econometrics* **70**(1), 9–38.
- Bai, J. (1994), 'Least squares estimation of a shift in linear processes', *Journal of Time Series Analysis* **15**(5), 453–472.
- Bai, J. (1997), 'Estimation of a change point in multiple regression models', *Review of Economics and Statistics* **79**(4), 551–563.
- Bai, J. and Perron, P. (1998), 'Estimating and testing linear models with multiple structural changes', *Econometrica* **66**(1), 47–78.
- Bai, Y. and Safikhani, A. (2022), 'A unified framework for change point detection in high-dimensional linear models', *arXiv preprint arXiv:2207.09007* .
- Baranowski, R., Chen, Y. and Fryzlewicz, P. (2019), 'Narrowest-over-threshold detection of multiple change points and change-point-like features', *Journal of the Royal Statistical Society: Series B (Statistical Methodology)* **81**(3), 649–672.
- Bulut, A., Singh, A. K., Shin, P., Fountain, T., Jasso, H., Yan, L. and Elgamal, A. (2005), Real-time nondestructive structural health monitoring using support vector machines and wavelets, in 'Advanced Sensor Technologies for Nondestructive Evaluation and Structural Health Monitoring', Vol. 5770, SPIE, pp. 180–189.
- Chang, P.-C., Fan, C.-Y. and Liu, C.-H. (2008), 'Integrating a piecewise linear representation method and a neural network model for stock trading points prediction', *IEEE Transactions on Systems, Man, and Cybernetics, Part C (Applications and Reviews)* **39**(1), 80–92.

- Chen, J. and Gupta, A. K. (2012), ‘Parametric statistical change point analysis: with applications to genetics’, *Medicine, and Finance. Springer* .
- Cheng, D., He, Z. and Schwartzman, A. (2020), ‘Multiple testing of local extrema for detection of change points’, *Electronic Journal of Statistics* **14**(2), 3705–3729.
- Cheng, D. and Schwartzman, A. (2015), ‘Distribution of the height of local maxima of gaussian random fields’, *Extremes* **18**(2), 213–240.
- Cheng, D. and Schwartzman, A. (2017), ‘Multiple testing of local maxima for detection of peaks in random fields’, *The Annals of Statistics* **45**(2), 529–556.
- Ding, Y., Yang, X., Kavs, A. J. and Li, J. (2010), A novel piecewise linear segmentation for time series, in ‘2010 The 2nd International Conference on Computer and Automation Engineering (ICCAE)’, Vol. 4, IEEE, pp. 52–55.
- Frick, K., Munk, A. and Sieling, H. (2014), ‘Multiscale change point inference’, *Journal of the Royal Statistical Society: Series B (Statistical Methodology)* **76**(3), 495–580.
- Fryzlewicz, P. (2014), ‘Wild binary segmentation for multiple change-point detection’, *The Annals of Statistics* **42**(6), 2243–2281.
- Fryzlewicz, P. (2023), ‘Narrowest significance pursuit: inference for multiple change-points in linear models’, *Journal of the American Statistical Association* (just-accepted), 1–25.
- Hann, C. E., Singh-Levett, I., Deam, B. L., Mander, J. B. and Chase, J. G. (2009), ‘Real-time system identification of a nonlinear four-story steel frame structure—application to structural health monitoring’, *IEEE Sensors Journal* **9**(11), 1339–1346.
- Hao, N., Niu, Y. S. and Zhang, H. (2013), ‘Multiple change-point detection via a screening and ranking algorithm’, *Statistica Sinica* **23**(4), 1553.

- Heinonen, M., Mannerström, H., Rousu, J., Kaski, S. and Lähdesmäki, H. (2016), Non-stationary gaussian process regression with hamiltonian monte carlo, *in* ‘Artificial Intelligence and Statistics’, PMLR, pp. 732–740.
- Huber, P. J. (2004), *Robust statistics*, Vol. 523, John Wiley & Sons.
- Hung, Y., Wang, Y., Zarnitsyna, V., Zhu, C. and Wu, C. J. (2013), ‘Hidden markov models with applications in cell adhesion experiments’, *Journal of the American Statistical Association* **108**(504), 1469–1479.
- Hyun, S., Lin, K. Z., G’Sell, M. and Tibshirani, R. J. (2021), ‘Post-selection inference for changepoint detection algorithms with application to copy number variation data’, *Biometrics* **77**(3), 1037–1049.
- Khan, F., Ghaffar, A., Khan, N. and Cho, S. H. (2020), ‘An overview of signal processing techniques for remote health monitoring using impulse radio uwb transceiver’, *Sensors* **20**(9), 2479.
- Kharinov, M. (2014), ‘Image segmentation using optimal and hierarchical piecewise-constant approximations’, *Pattern recognition and image analysis* **24**(3), 409–417.
- Lavielle, M. (2005), ‘Using penalized contrasts for the change-point problem’, *Signal processing* **85**(8), 1501–1510.
- Li, H., Munk, A. and Sieling, H. (2016), ‘Fdr-control in multiscale change-point segmentation’, *Electronic Journal of Statistics* **10**(1), 918–959.
- Liao, S. X. and Pawlak, M. (1996), ‘On image analysis by moments’, *IEEE Transactions on Pattern analysis and machine intelligence* **18**(3), 254–266.
- Lu, J., Zheng, X., Sheng, Q. Z., Hussain, Z., Wang, J. and Zhou, W. (2019), Mfe-har: multiscale feature engineering for human activity recognition using wearable sensors, *in* ‘Proceedings of the

- 16th EAI International Conference on Mobile and Ubiquitous Systems: Computing, Networking and Services’, pp. 180–189.
- Olshen, A. B., Venkatraman, E. S., Lucito, R. and Wigler, M. (2004), ‘Circular binary segmentation for the analysis of array-based dna copy number data’, *Biostatistics* **5**(4), 557–572.
- Pein, F., Sieling, H. and Munk, A. (2017), ‘Heterogeneous change point inference’, *Journal of the Royal Statistical Society: Series B (Statistical Methodology)* **79**(4), 1207–1227.
- Perron, P. (1989), ‘The great crash, the oil price shock, and the unit root hypothesis’, *Econometrica: journal of the Econometric Society* pp. 1361–1401.
- Phoon, K.-K., Huang, H. and Quek, S. T. (2005), ‘Simulation of strongly non-gaussian processes using karhunen-loeve expansion’, *Probabilistic engineering mechanics* **20**(2), 188–198.
- Schwartzman, A., Gavrilov, Y. and Adler, R. J. (2011), ‘Multiple testing of local maxima for detection of peaks in 1d’, *Annals of statistics* **39**(6), 3290.
- Tebaldi, C. and Lobell, D. (2008), ‘Towards probabilistic projections of climate change impacts on global crop yields’, *Geophysical Research Letters* **35**(8).
- Tomé, A. and Miranda, P. (2004), ‘Piecewise linear fitting and trend changing points of climate parameters’, *Geophysical Research Letters* **31**(2).
- Van Laerhoven, K., Berlin, E. and Schiele, B. (2009), Enabling efficient time series analysis for wearable activity data, in ‘2009 International Conference on Machine Learning and Applications’, IEEE, pp. 392–397.
- Vostrikova, L. Y. (1981), Detecting “disorder” in multidimensional random processes, in ‘Doklady Akademii Nauk’, Vol. 259, Russian Academy of Sciences, pp. 270–274.
- Yao, Y.-C. and Au, S.-T. (1989), ‘Least-squares estimation of a step function’, *Sankhyā: The Indian Journal of Statistics, Series A* pp. 370–381.

Yu, M. and Ruggieri, E. (2019), 'Change point analysis of global temperature records', *International Journal of Climatology* **39**(8), 3679–3688.